PAPER

Development and metrological applications of Josephson arrays at PTB

Meas. Sci. Technol. **23** (2012) 124002 (19pp) doi:10.1088/0957-0233/23/12/124002

Development and metrological applications of Josephson arrays at PTB

Ralf Behr, Oliver Kieler, Johannes Kohlmann, Franz Müller and Luis Palafox

Physikalisch-Technische Bundesanstalt (PTB), Bundesallee 100, D-38116 Braunschweig, Germany

E-mail: luis.palafox@ptb.de and johannes.kohlmann@ptb.de

Received 13 April 2012, in final form 1 August 2012
Published 19 November 2012
Online at stacks.iop.org/MST/23/124002

Abstract
The discovery of the Josephson effects 50 years ago initiated a revolution for electrical voltage metrology. This revolution started with single Josephson junctions delivering a few millivolt at most. Meanwhile, highly integrated series arrays containing more than 10 000 or even 300 000 junctions have been developed and fabricated for output voltages up to 10 V. Josephson voltage standards are nowadays used in many laboratories worldwide for dc applications. After their adoption for the representation of the unit of voltage in 1990, the focus of research shifted towards programmable Josephson series arrays. The increasing interest in highly precise ac voltages resulted in new developments for their metrological applications in the last 15 years. This paper summarizes the principal contributions from PTB to the present state of Josephson voltage standards with particular focus on developments and applications for ac standards in metrology and our proof-of-concept demonstrations. The presentation includes the two most promising versions of ac standards, being the programmable Josephson voltage standard based on binary divided series arrays and the Josephson arbitrary waveform synthesizer based on a pulse-driven series array.

Keywords: dc and ac Josephson voltage standards, Josephson junction series arrays, SINIS and SNS Josephson junctions, quantum voltmeter, impedance measurement, characterization of analogue to digital converters, programmable Josephson voltage standards, Josephson arbitrary waveform synthesizer, ac–dc transfer, thermal converter, digital to analogue converter

(Some figures may appear in colour only in the online journal)

1. Introduction

One of the aims of this special feature is to celebrate the 50th anniversary of the publication of Josephson's seminal paper in 1962. Fifty years later, the Josephson effect is firmly established as a macroscopic quantum effect. Josephson's predictions were confirmed within a year and have become the basis for many applications (cf Anders *et al* 2010). Shapiro (1963) experimentally measured steps of constant voltage by irradiating single junctions with microwaves. These steps have become the basis for the representation of voltage and marked the start of a revolution for voltage standards. Today, series arrays with up to 300 000 Josephson junctions (JJs) for metrological applications are routinely manufactured at no less than six locations around the world. The voltage of the Shapiro steps has risen by six orders of magnitude from tens of μV to 10 V.

Numerous review papers have been published covering the principal application of the Josephson effect in metrology, Josephson voltage standards (JVSs) (cf Harris and Niemeyer 2011, Kohlmann and Behr 2011, Jeanneret and Benz 2009, Benz and Hamilton 2004, Kohlmann *et al* 2003, Behr *et al* 2002, Hamilton 2000) as well as the physics underpinning these standards (cf Kautz 1992, 1996). In this paper we will summarize the main contributions that the Physikalisch-Technische Bundesanstalt (PTB) has made to the development and deployment of programmable Josephson arrays in metrology. The contributions from other groups are covered in additional papers in this special feature.

A brief historical overview of the developments that led to programmable Josephson arrays will be given in

section 2, which will also introduce the underlying physics as required. Section 3 will concentrate on the developments in fabrication technology that have made possible the metrological applications, covered in section 4. A separate section is dedicated to pulse driven Josephson arrays, due to the many differences that they present. The conclusions and a short outlook will follow in section 6.

2. From single junctions to Josephson waveforms

In this section, we will follow the evolution from single JJs to today's series arrays with many thousands of junctions. Detailed descriptions of the Josephson effects and JJs have been given in several reviews (e.g. Josephson 1965, Kautz 1992, Rogalla 1998) and textbooks (e.g. Barone and Paternò 1982, Likharev 1986, Kadin 1999).

As already mentioned in the introduction and elsewhere in this special feature, in 1962 Brian Josephson[1] laid the foundation for what would become a revolution in the field of electrical high-precision measurements, among other applications (Josephson 1962). Brian Josephson was awarded one half of the 1973 Nobel prize for physics for his paper. Josephson's predictions were met with disbelief initially (cf McDonald 2001), but were experimentally confirmed within a year. Using the BCS theory by Bardeen *et al* (1957), Josephson predicted two effects due to tunnelling of Cooper pairs between two superconductors weakly coupled: the dc and the ac Josephson effects. The dc Josephson effect predicts that a dc supercurrent can flow across the junction at zero voltage. The supercurrent is determined by the phase difference ϕ between the two wavefunctions on each side of the link; $I = I_c \sin\phi$, where I_c denotes the critical current. The ac Josephson effect describes the behaviour of the junction with a finite voltage V applied across the weak link. An ac supercurrent of frequency

$$f_J = (2e/h)V, \tag{1}$$

where e is the elementary charge and h is Planck's constant, occurs in addition to the dc current. Josephson's predictions have become the basis for the representation of the volt, namely that an external signal of frequency f can phase lock this phase oscillation and result in steps of constant voltage at

$$V_n = n(h/2e)f = n\Phi_0 f, \tag{2}$$

with Φ_0 the magnetic flux quantum and $n = 0, \pm 1, \pm 2, \ldots$, the integer step number. These steps were observed by Shapiro (1963) for the first time and are thus often called Shapiro steps. Equation (2) is also often written as $V_n = nK_J^{-1}f$, with the quotient $K_J = 2e/h$ named the Josephson constant.

Josephson's original work studied the tunnelling of Cooper pairs through an insulating material weakly linking two superconductors, in an SIS junction (superconductor–insulator–superconductor). Josephson also mentioned that the same behaviour should be observed when a normal conductor is used as the weak link in an SNS junction. We will also mention SINIS junctions in this paper, with two insulating barriers on both sides of the normal conductor.

[1] In 1962, Brian D Josephson was a 22 year old graduate student at Trinity College in Cambridge, UK.

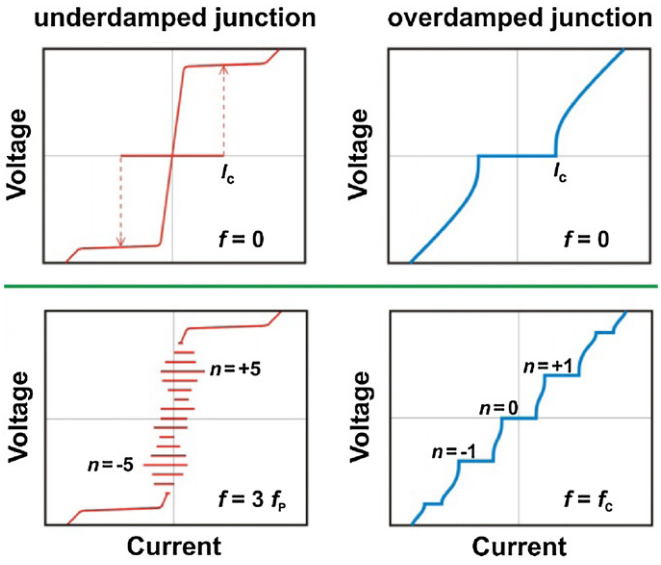

Figure 1. Schematic current–voltage characteristics of underdamped (left) and overdamped (right) JJs without (top) and with (bottom) microwave irradiation. Some constant-voltage steps are marked. The microwave power is adjusted for optimized operation in each case.

The dynamics of the JJ are often described using the resistively-capacitively-shunted-junction (RCSJ) model (Stewart 1968, McCumber 1968). In this model, the real JJ of area A is represented by an ideal Josephson element (Josephson inductance) shunted by an ohmic resistance R and a capacitance C. The electrical behaviour and the type of junction can be characterized by the dimensionless McCumber parameter, equal to the square of the quality factor of the LCR resonator, $\beta_c = Q^2 = (2\pi f_p RC)^2$, where f_p is known as the plasma frequency and is determined by the junction parameters. In detail, $f_p = (ej_c/\pi hC_s)^{1/2}$, where j_c is the critical current density and $C_s = C/A$ is the specific junction capacitance. Figure 1 shows the different I–V characteristics (IVCs) of underdamped junctions, with $\beta_c > 1$, and overdamped junctions with $\beta_c \leqslant 1$. Overdamped junctions present a single-valued IVC. The desired constant-voltage steps are induced when microwave power is applied. Strongly underdamped junctions ($\beta_c \gg 1$) present hysteretic IVCs without microwaves. Under irradiation at low power, multiple Shapiro steps are possible for the same bias current (Levinsen *et al* 1977).

2.1. Josephson series arrays for dc voltage standards

For the representation of the unit of voltage, equation (2) describes a perfect frequency to voltage converter. Microwaves with frequencies in the GHz range can be referenced to an atomic clock and finely tuned, locked and reproduced to the level of a few parts in 10^{11} or better. Taylor *et al* suggested in (1967) using Shapiro steps as the basis for voltage standards. The universality of the Josephson effect, proven with increasing accuracy from Clarke (1968) to Jain *et al* (1987) to parts in 10^{19}, was another crucial aspect for the establishment of JVSs. In the 1970s, leading National Metrology Institutes (NMI) started to use single JJs

delivering typically 10 mV for dc voltage metrology. This work culminated with a series array of 20 JJs, which were individually biased and delivered an output voltage of about 100 mV (Endo *et al* 1983).

Considerable efforts worldwide were devoted to matching the 1.018 V provided by the voltage standard established at that time, based on Weston cadmium standard cells (cf for example Hamilton (2000)). As the order of the step n cannot be indefinitely increased, the efforts were directed at what are known as series arrays of JJs. In these arrays, the JJs are connected in series for the output voltage. The voltage across the complete array can only be quantized when every junction in the array ($i = 1, 2, \ldots, m$) sits on an individual Shapiro step of order n_i. Equation (2) can thus be rewritten as

$$V_{n,m} = \sum_{i=1}^{m} n_i \Phi_0 f, \tag{3}$$

to illustrate the specific transfer of n_i flux quanta Φ_0 through each of the m JJs during one period of the frequency f.

The IVC of each JJ in the series array still depends on the junction parameters and on the microwave power that it receives. As will be explained in detail in section 3, the limitations for series arrays due to the fabrication spread of junction parameters and the inhomogeneous microwave power distribution were solved for the first time by a cooperation between the American National Institute of Standards and Technology (NIST) and PTB (Niemeyer *et al* 1984) that exploited the suggestion from Levinsen *et al* (1977). This combination of new concepts and ideas achieved voltages slightly above 1 V and matched the voltage of Weston cells. The series array incorporated 1474 SIS JJs irradiated at 70 GHz and operated on their fifth Shapiro step on average.

Before the 1980s ended, both NIST (Lloyd *et al* 1987) and PTB (Pöpel *et al* 1990) independently fabricated arrays capable of generating 10 V, with up to 20 000 JJs. Operation at much lower frequencies was also demonstrated by the group at Jena University (Müller *et al* 1990) and later on at NIST (Hamilton *et al* 1991). They reached 1 V with 35 and 24 GHz microwaves, respectively.

Reviews of the developments up to this time are given for example by Niemeyer (1989), Kautz (1992) and Pöpel (1992). These SIS arrays with multiple Shapiro steps led to the adoption of JVSs for the representation of the volt on 1 January 1990 (Quinn 1989). Today, about 50 JVSs are in operation at NMI, calibration laboratories (Wood and Solve 2009) and instrumentation manufacturers (e.g. Giem 1991). As Wood and Solve show, all the systems that operate at the 10 V level provide a combined uncertainty of between a few parts in 10^{10} and a few parts in 10^{11}. A significant factor in the adoption of the JVS was the commercial availability of turn-key systems. A number of companies have offered these over the years; to the best of our knowledge, only Hypres and Supracon[2] offer such systems at present.

[2] Hypres Inc., USA: www.hypres.com, and Supracon AG, Germany: www.supracon.com.

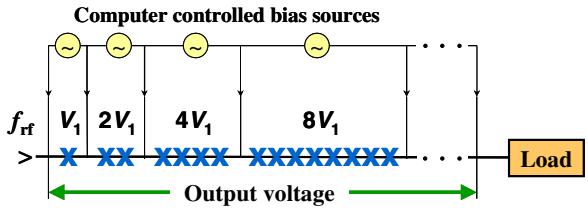

Figure 2. Schematic design of a PJVS based on a binary series array of JJs (shown as X). The series array is operated as a multi-bit DAC.

2.2. Programmable Josephson series arrays for 1 V and 10 V

Due to the overlapping Shapiro steps of SIS arrays, the time required to set the array voltage to a desired level is not deterministic. The road to deterministically programming the output voltage of a Josephson array started with Hamilton *et al* in 1995. They divided the biasing connection in a series array of overdamped JJs into individual segments, as depicted in figure 2. The resulting 'digital to analogue converter (DAC) with fundamental accuracy' was implemented using externally shunted SIS junctions and demonstrated voltages between ± 77 mV with 0.15 mV resolution.

Practical considerations dictate a change of Josephson technology for these quantum accurate DACs in order to achieve output voltages of 1 V or higher. Two distinct routes to single-valued IVCs towards 10 V at reasonable microwave power levels were pursued: using SNS and SINIS junctions. Their IVCs under microwave irradiation are determined by the product of the critical current I_c and the resistance of the junction in the normal state R_n. According to equation (1), this characteristic voltage $V_c = I_c R_n$ results in a characteristic frequency f_c for the junction. The width and stability of the Shapiro steps are optimal when the junctions are operated close to f_c (cf Kautz 1995).

These arrays are often called programmable Josephson arrays or programmable Josephson voltage standards (PJVSs) to explicitly indicate their deterministic steps. One possibility is to subdivide the complete series array into subarrays with 2^k JJs, in which case they are also called binary Josephson arrays. When the bias conditions of these segments or subarrays are changed in time among the quantum steps (normally 0, +1 or −1), equation (3) opens the possibility of generating time-varying voltages across a Josephson array, $V(t) = M(t)\Phi_0 f$, where $M(t)$ represents the sum of the products of each step order multiplied by the number of junctions biased on that step.

Rapid progress followed after the proof-of-concept experiment (Hamilton *et al* 1995) and NIST demonstrated a 1 V PJVS with 32 768 SNS junctions operated at 16 GHz (Benz *et al* 1997). At PTB, SINIS junctions operated at 70 GHz were chosen as the required $I_c R_n$ products were achievable. In addition, only small changes to the microwave design from SIS arrays were required. Furthermore, 'just' 70 000 junctions are required for 10 V. A supplementary advantage was the limited process differences from the mature SIS manufacturing technology and also that the same materials were used. Binary arrays with 8192 SINIS junctions for output voltages slightly above 1 V were fabricated in 1999 (Behr *et al* 1999) and 10 V

just a few months later, although divided into only 6 segments (Schulze *et al* 2000). A SINIS array for 10 V with 18 segments was demonstrated in 2006 (Müller *et al* 2007). PTB reproduced this result with SNS arrays manufactured in cooperation with NIST for operation at 70 GHz for 1 and 10 V two years later (Mueller *et al* 2009). NIST and the Japanese National Institute of Advanced Industrial Science and Technology (AIST) have also reported 10 V programmable SNS arrays, both operated at around 20 GHz (Yamamori *et al* 2008, Dresselhaus *et al* 2011). The applications in metrology of these binary arrays are detailed in section 4.

Before reviewing the technological developments that enabled this quick transition from hysteretic SIS arrays to binary quantum DACs, we would like to mention a radically different approach to the generation of ac waveforms using Josephson arrays.

2.3. Pulse driven Josephson arrays

Most JVSs are operated with sinusoidal microwaves to affect the transfer of flux quanta through the JJs (cf equation (3)). This mode of operation works well if the microwave frequency is close to the characteristic frequency of the junctions, as shown by simulations (Monaco 1990, Maggi 1995, Kautz 1995, Benz and Hamilton 1996). The change in output voltage that can be achieved by modulating the microwave frequency is however limited. Large variations of the array voltage can nevertheless be achieved if the JJs are operated by a train of short current pulses, as demonstrated for the first time by Benz and Hamilton (1996). The width of the constant-voltage steps is nearly independent of the pulse repetition frequency between zero and the characteristic frequency f_c, if the rise and fall times of the pulses are short compared to $1/f_c$ (10 GHz corresponds to 100 ps). For a given pulse area, each pulse transfers a single flux quantum through the barrier. The repetition frequency of the pulses then determines the voltage across the array. This repetition frequency can be modulated to generate a waveform in the Josephson arbitrary waveform synthesizer (JAWS), as suggested by Benz and Hamilton (1996). The initial realization employed SNS junctions for an output voltage below 1 mV and sinusoidal waveforms with spectral purity better than –100 dBc in the signal band. The NIST group has continuously improved the implementation of their original idea and they recently reached output voltages of 275 mV (rms) (Benz *et al* 2009a). Nevertheless, 1 V is still a real challenge. A pulse drive based on short optical pulses has also been investigated (Williams *et al* 2004, Urano *et al* 2010). An advantage of this approach based on balanced photodiodes is that it is rather easily extendable for operation of parallel arrays as a route towards higher output voltages (cf Kohlmann *et al* 2006). Further details of the work at PTB with pulse driven arrays are given in section 5.

3. Development of JJ series arrays

In this section, we will concentrate on the microfabrication and design developments that made possible the transition from the combination of a few individually biased JJs and a voltage divider to programmable 10 V series arrays.

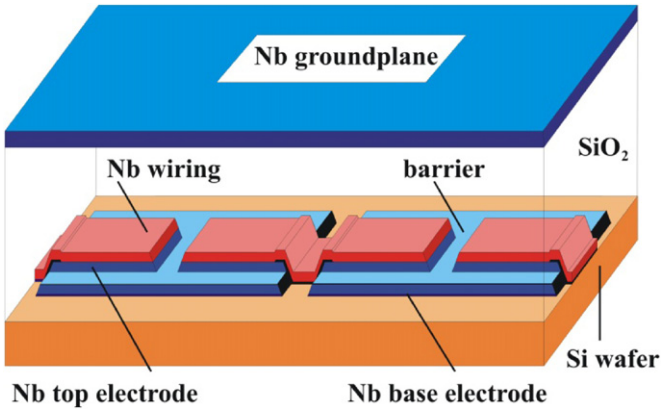

Figure 3. Array of inline junctions (SIS or SINIS) as an integrated part of a microstrip transmission line. The Nb-ground can be placed above the array, as shown, or underneath.

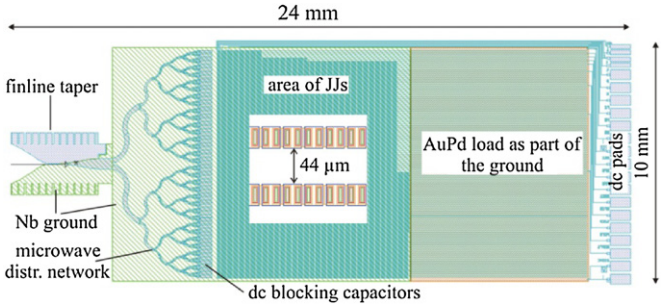

Figure 4. Microwave design of a programmable 10 V SNS circuit ($N = Nb_xSi_{1-x}$) operating at 70 GHz. The inset picture shows enlarged details of two parallel microstrips.

3.1. Conventional SIS JVSs

As mentioned in section 2, the use of strongly underdamped, SIS JJs, suggested by Levinsen *et al* (1977), was an important step towards series arrays with practical output voltages. For junctions with much higher McCumber parameters than had been employed previously, $\beta_c \approx 10^5$, Shapiro steps in the vicinity of zero bias can occur and overlap almost completely. It is sufficient to fix the operating point of each junction on one of these steps, which can be of different order as operating points between the steps do not exist! As a result, it was possible to tolerate a reasonably large parameter spread (I_c, R_n) of the SIS junctions and to bias the array with only one dc current source.

The IVC of each junction in the series array still depends on the microwaves. For a single rf drive, a nearly homogeneous power distribution over the whole array is an essential requirement to further increase the number of junctions. Therefore the integration of the SIS junction array in a planar superconducting microstripline (figure 3) was a milestone towards voltage standards operating at 1 and 10 V. The microstrip is coupled to a standard 70 GHz rectangular waveguide via an antipodal finline taper or antenna (cf figure 4). A cooperation between PTB and NIST successfully demonstrated this principle (Niemeyer *et al* 1984) by means of a series array consisting of 1474 SIS junctions (PbInAu–PbO_x–PbAu). For the first time, a Josephson voltage larger

Table 1. Design parameters of 10 V circuits fabricated at PTB for the classical (JVS) and the programmable (PJVS) Josephson voltage standard operated at 70 GHz.

Parameter	SIS[a] (JVS)	SINIS[b] (PJVS)	SNS[c] (PJVS)
Number of JJs	13 924	69 632	69 632
Number of microstrips	4	128	128
Number of JJs in one microstrip	3481	136–562	136–582[d]
Junction length l (μm)	20	15	6
Junction width w (μm)	50	30	20
Microstrip impedance Z_0 (Ω)	6	8	9
Current density j_c (A cm^{-2})	10	750	3000
Critical current I_c (mA)	0.1	3.5	3.5
Normal state resistance R_n (Ω)	15 at 1.5 mV	0.04 (at $2I_c$)	0.04 (at $2I_c$)

[a] Nb–Al/AlO_x–Nb.
[b] Nb–Al/AlO_x/Al/AlO_x/Al–Nb.
[c] Nb–Nb_xSi_{1-x}–Nb with $x \approx 10\%$.
[d] In contrast to SINIS, the number of JJs in some microstrips is slightly different.

than 1 V was generated. Considerable efforts to improve the design and fabrication technology for operation at 70 GHz were still required in order to attain the magic goal of 10 V and to realize practical JVSs. NIST preferred the Nb–Nb_2O_5–PbInAu technology and reported the first 10 V circuit with 14 184 junctions in 1987 (Lloyd *et al* 1987). Two years later PTB fabricated its first 10 V chip with more than 20 000 JJs using the Nb–Al/AlO_x–Nb technology (Pöpel *et al* 1990).

In the 1990s all manufacturers of 10 V SIS series arrays adopted designs for the frequency range from 70 to 75 GHz. At nearly the same time, the reliable Nb–Al/AlO_x–Nb technology developed by Gurvitch *et al* (1983a) became the predominant fabrication process. At PTB both this technology and the design were continuously improved to increase the fabrication yield of 10 V chips. High quality dc characteristics and improved microwave response were achieved by 'turning the design upside down'. As shown in figure 3, the Nb–Al/AlO_x–Nb trilayer was deposited directly onto the polished Si wafer, followed by the dielectric layer and the ground plane on top of the junction arrays (instead of underneath) (cf Müller *et al* 1995). The final version of the SIS 10 V JVS circuits developed at PTB (Müller *et al* 1997) consisted of 13 924 JJs arranged in four microwave microstrips connected in parallel (see also table 1). In the dc circuit, which includes the output connections and the bias leads and is galvanically isolated from the microwave circuit, all the JJs are connected in series. Starting in 1997 the PTB fabrication technology, called the modified self-aligned whole wafer process, and based on inline junctions with minimized parasitic capacitances (Müller *et al* 1995), was transferred to IPHT in Jena and finally from there to the company Supracon. This is one of the commercial providers of JVSs mentioned in section 2.

3.2. Programmable JVSs

The interest in extending the use of JVSs from dc to ac initiated the development of PJVSs in the mid 1990s. For their first approach Hamilton *et al* (1995) used externally shunted SIS junctions as overdamped Josephson contacts. This type of junction was abandoned shortly afterwards, due to the external shunt resistance and its large parasitic inductance, which creates microwave-design problems and additional fabrication difficulties. The technological focus moved to arrays of intrinsically shunted JJs such as SNS and SINIS. When NIST started as the first NMI to implement SNS junctions (Benz 1995), the low resistivity of the normal-conducting barrier materials commonly used at that time required a 'low' frequency drive around 15 GHz. Materials such as AuPd, HfTi or later on TiN_x allow only 'low' I_cR_n products (I_c: critical current, R_n: normal state resistance) of the junctions, typically between 10 and 40 μV when deposited to reasonable thicknesses for the micrometer-sized junctions commonly used at the time. Nevertheless NIST and AIST succeeded in the fabrication of such programmable circuits (Benz *et al* 1997, Yamamori *et al* 2006). However, the large number of junctions required to reach 10 V when operated from 15 to 20 GHz remains a challenge for this technology.

PTB followed an alternative route and explored SINIS junctions for PJVSs (Schulze *et al* 1998). Arrays of these junctions can use the same 70 GHz microwave drive as conventional SIS JVSs, established throughout the 1990s. This is possible because the I_cR_n product of SINIS junctions can be tuned over a relatively large frequency range. The higher microwave frequency translates into a reduction in the number of junctions and the microwave design could be carried over. In addition, the array fabrication is based, except for some minor modifications, on the same reliable Nb–Al standard technology that was well established for conventional SIS JVSs (Müller *et al* 2001). As a result, PTB progressed very quickly from 1 V (Behr *et al* 1999) to the first 10 V SINIS PJVS circuits (Schulze *et al* 2000). However, their limited resolution of six segments and a step width of only 200 μA restricted their applications to fast and simplified dc voltage calibrations.

After optimizing the microwave design with shorter microstrips, as detailed in section 3.3 (cf table 1), and further improving the fabrication process (double-insulated trilayer edges), PTB produced in 2006 the first ever 10 V binary arrays in SINIS technology using Nb–Al/AlO_x–Nb. The large step width achieved (>600 μA) made these arrays immediately suitable for applications in dc and ac metrology (Müller *et al* 2007). The new 10 V chips with 69 632 series-connected SINIS junctions were divided into 18 segments. However, the very thin AlO_x barriers are easily damaged by the plasma processes in the fabrication, leading to a low yield of only 5% for 10 V arrays. For this reason, PTB was always seeking another barrier material and evaluating its suitability for a programmable SNS version that would enable higher production yield and that could be used as a drop-in replacement for existing 70 GHz SIS or SINIS systems. The barrier material finally found was the 'rediscovered' amorphous Nb_xSi_{1-x}. The resistivity of this material, already known since 1987 as a candidate for JJs (Barrera and Beasley 1987), can be tuned by its Nb

content from insulating to conducting (metallic). It therefore represents an almost universal N barrier for SNS junctions. For instance NIST started using Nb_xSi_{1-x} barriers for SNS arrays driven at 20 GHz in 2006 (Baek *et al* 2006). In close cooperation between PTB (design and circuit fabrication) and NIST (trilayer deposition) it was successfully demonstrated that a 70 GHz drive is also possible for a special composition of Nb_xSi_{1-x}. This cooperation realized the first 10 V PJVSs with Nb_xSi_{1-x} barrier junctions in 2008 (Mueller *et al* 2009). These circuits driven at 70 GHz show an improved performance (current margins larger than 1 mA) and for the first time no 'missing junctions', as compared to 10 V SINIS arrays. Their fabrication technology has much better yield, most likely because plasma process-induced damage of the barrier is eliminated. Further details of the design and fabrication of these programmable arrays are given in section 3.3.

Encouraged by these results, PTB has been fabricating completely in-house 10 V SNS circuits comprising 69 632 JJs with a Nb_xSi_{1-x} barrier since 2010. Also in 2010, NIST reported their first 10 V arrays with about 300 000 triple-stacked junctions and the same barrier material, but tuned for frequencies from 16 to 20 GHz (Dresselhaus *et al* 2011). A third 10 V Josephson series array was developed by AIST (Yamamori *et al* 2008), with more than 300 000 double-stacked NbN–TiN_x–NbN junctions operated at 16 GHz and 10 K.

3.3. Design and fabrication of PJVSs with Nb_xSi_{1-x} barriers for 70 GHz

As already pointed out, the homogeneous distribution of microwave power to all the JJs in a series array is a crucial aspect of their design. Guidelines for the design of series arrays embedded in microstrip transmission lines were already established for conventional SIS JVSs (Kautz 1992). Supplemented by some special design principles for nonhysteretic JJs (Kautz 1995), they are mostly valid for programmable circuits operated at 70 GHz. The microwave designs for 70 GHz PJVS are based on conventional SIS designs and are almost identical for SNS and SINIS circuits. Only the junction area (lw, see table 1 for typical values) must be adapted to the larger current density of Nb–Nb_xSi_{1-x}–Nb junctions. Details have been described by Mueller *et al* (2009) and are summarized in table 1. The maximum number of JJs that can be embedded into one of the parallel-driven microstrip lines, in order to maintain an approximately constant microwave current, is the most important design parameter of the microwave circuit. This number is determined by the microwave attenuation of the microstrip and mainly due to losses from the embedded junctions. Programmable arrays need to operate for all possible bias patterns, from a single biased JJ and all other on the zero-order Shapiro step to the whole array operating collectively, ideally with the same bias currents. Unbiased junctions however attenuate microwave power considerably. This attenuation per JJ, estimated on the basis of the RCSJ model for a passive microstrip (Kautz 1992), is much larger for intrinsically shunted SINIS or SNS junctions than for SIS JJs. The estimated value is almost identical for SINIS and SNS junctions and amounts to 0.04 dB per JJ (Mueller *et al* 2009). In order to keep the attenuation below 6 dB for the 'last' junction, a maximum of 150 JJs can be integrated into a single microstrip. Our investigations with SINIS arrays showed that self-oscillation coupling effects between the JJs in active microstrips (first-order Shapiro steps) partly compensate for the large attenuation (Behr *et al* 1999). Therefore, microstrips with more JJs can be used for the larger segments in the array, as all the JJs in each microstrip are always biased to the same Shapiro step. The self-excitation effect is well described by the virtual model of Kim *et al* (2006). As a result, from the low potential connection of the array, the segments are initially organized in decreasing order of junctions (68, 34, 17, 8, 4, 2, 1, 1 and 1 in the case of a 10 V array). From that point on, the sequence follows the 'natural' order (136, 272, . . .).

All programmable circuits developed at PTB have an exactly binary sequence, or approximately binary in the 10 V case, for the number of junctions in the array segments. Figure 4 shows the design of a programmable 10 V array. Due to the needed connections and the increased microwave attenuation of unbiased array segments just mentioned, the smallest segments are placed in one of the outermost microstrips (top in figure 4). The current margins attainable for the Shapiro steps are limited by the segment with 68 junctions at the end of the first microstrip together with the largest 'array microstrips' with 582 JJs. These large microstrips are always biased together and profit from the self-oscillation effects described above. The shortest microstrip is determined by the maximum attenuation for the segment furthest from the antenna. Depending on the bias pattern for the complete array, the segment with 68 JJs can lay behind up to another 68 unbiased JJs. The number of microstrips connected in parallel for the microwaves, 128 for the 10 V design, is a compromise between tolerable attenuation (including self-excitation) and available power at 70 GHz.

Besides the primary design goal of maintaining nearly the same microwave power for all JJs, the circuit area containing all junctions should be concentrated as much as possible to minimize the parameter spread. For this reason, dc connections to the array segments have been restricted to the ends of the microstrips and to one of the two outermost microstrips. All these practical considerations resulted in a 'homogeneous' 1 V design with 128 JJs in each microstrip and an 'inhomogeneous' 10 V design (figures 4 and 5). The 69 632 junctions of the 10 V design are subdivided into 18 segments with different numbers of JJs per microstrip: 4 microstrips with 136 JJs, 2 with 272 JJs, and 122 microstrips with between 544 JJs and 582 JJs. All microstrips are extended beyond the array length with superconducting wires in order to reach the microwave termination and to match all the lengths. The superconducting ground plane (Nb) is, as already mentioned, deposited on top of the SNS arrays. A 1 μm thick SiO_2 layer acts as the dielectric in the microstrip. The microwave termination of the array microstrips is realized by a distributed resistive plane from AuPd at the end of the ground plane.

SNS circuits for the PJVSs are patterned from Nb–Nb_xSi_{1-x}–Nb trilayers deposited by dc sputtering onto

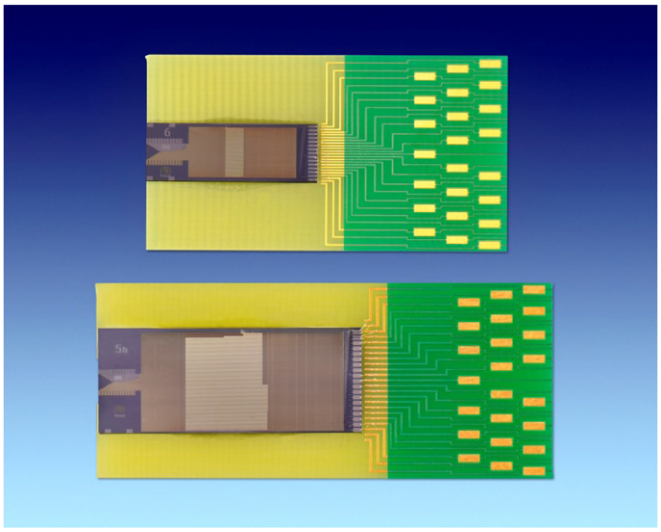

Figure 5. Photograph of programmable voltage standard circuits for operation at 70 GHz mounted on special chip carriers. At the top: 1 V circuit with a chip size of 15 mm × 5.5 mm and the 10 V circuit (24 mm × 10 mm) below.

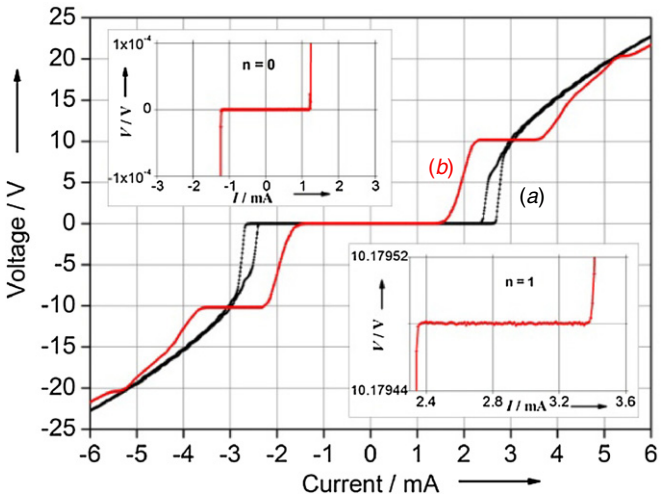

Figure 6. IVC of a 10 V PJVS with 69 632 SNS junctions, (*a*) without microwaves, (*b*) with microwaves at 70.7 GHz and 60 mW at the antenna. The insets show the 10 V step ($n = 1$) and the zero voltage step ($n = 0$) with high resolution. Junction parameters: $I_c = 2.7$ mA; $I_cR_n = 155\ \mu$V (at $2I_c$).

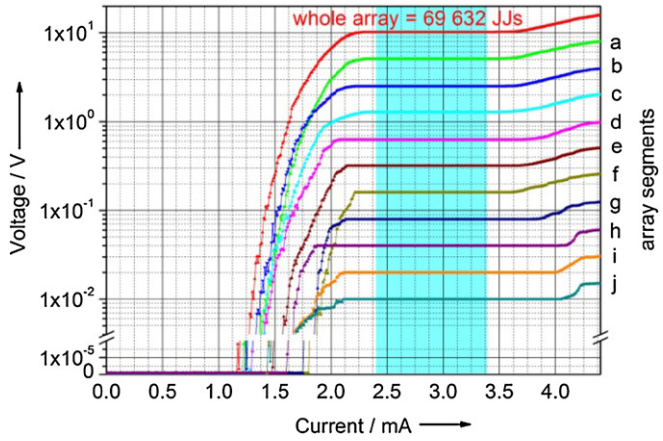

Figure 7. IVC of a complete 10 V array and of different array segments under microwave irradiation at 70.7 GHz and 60 mW at the antenna. For clarity, the smallest segments were grouped for curve (j). The number of JJs in each segment decreases alphabetically from top to bottom: (a) 34 816, (b) 17 408, (c) 8704, (d) 4352, (e) 2176, (f) 1088, (g) 544, (h) 272, (i) 136 and (j) $1 + 1 + 1 + 2 + 4 + 8 + 17 + 34 = 68$ (half of first microstrip).

3 inch Si wafers. The growth of the normal-conducting Nb_xSi_{1-x} is the key step of the trilayer deposition, because both the thickness (≈10 nm) and the composition ($x \approx 10\%$) determine very sensitively j_c and I_cR_n of the SNS JJs. In order to achieve as well as possible the aims for I_c and R_n of a given design (cf table 1), the Nb_xSi_{1-x} barrier is co-sputtered in a separate chamber from two 2 inch targets (Nb and p-doped Si) in confocal position onto the rotating wafer. The trilayers are patterned by means of a conventional self-aligning process that is very similar, except for the barrier material, to the fundamental selective niobium etching process first developed by Gurvitch *et al* (1983b). With the exception of the Nb-ground plane and the AuPd-load resistor for the microwaves (as part of the ground plane), all metallic (Nb; NbSi) and insulating (SiO_2) layers are patterned with electron-beam (e-beam) lithography and inductively coupled plasma dry etching (cf Mueller *et al* 2009).

Figure 6 presents the IVC of a 10 V circuit without (*a*) and with microwave bias (*b*) for the case that the design values for I_cR_n and j_c are nearly fulfilled. The Shapiro steps $n = 0$ and $n = \pm 1$ extend, as demonstrated by the inset pictures, over a current range larger than 1 mA. Figure 7 shows the IVCs of the whole circuit and of nearly all segments of the (approximately) binary 10 V array under microwave irradiation. The large current margins (⩾1 mA) and the almost complete overlap allow selecting the same dc current bias for all the segments on steps $n = \pm 1$ (centred around $I_{dc} \approx \pm 3$ mA). Low bias currents at 10 V and a relatively small amount of microwave power are special features of the 10 V circuits manufactured by PTB. These properties result in a low thermal load and are advantageous for the use of cryo-coolers. The applications of these 1 and 10 V binary Josephson arrays, fabricated with a good yield at PTB, are covered in section 4.

4. Applications of binary Josephson arrays

Applications in metrology of binary Josephson arrays have been explored intensively over the last 10 years. For dc measurements it has been demonstrated that these arrays are superior to conventional arrays as they allow easier automation, faster polarity reversing and thus better uncertainties within a given measurement time (Burroughs *et al* 1999b, Behr *et al* 2001, 2003). A long-term automated measurement over 18 h proves the robustness and reliability of the programmable arrays. As can be seen in figure 8, the measurements for nearly 2500 polarity reversals at the 10 V level agree within ±4 nV (Palafox *et al* 2009).

Analysis of the Allan deviation (e.g. Witt 2005) for this data series shows that the measurements remain in the white noise regime even for this extended measurement

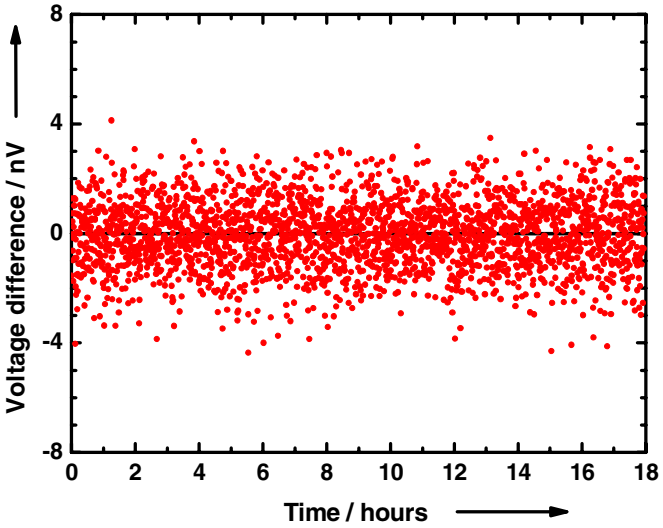

Figure 8. Long-term comparison of two 10 V SINIS arrays.

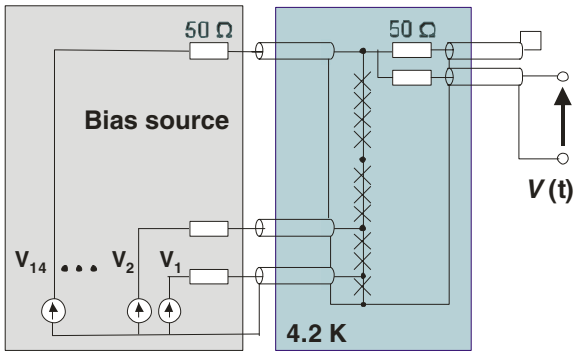

Figure 9. Schematic diagram of the JWS.

interval. The resulting relative difference of 5 pV V^{-1} with a type-A uncertainty of 3 pV V^{-1} from this fully automated comparison far exceeds the demands for the incorporation of the programmable Josephson arrays into ac electrical standards. Nevertheless, it indicates that a very low uncertainty can be reached within a short measuring time.

A typical setup for synthesizing Josephson waveforms is shown in figure 9. The Josephson array is operated at temperatures of 4.2 K, typically in a transportable liquid helium dewar and irradiated with 70 GHz microwaves (not shown). Each of the binary array segments can be independently set to the $n = 0, \pm 1$ steps by the fast programmable multi-channel bias source (Patel *et al* 2001). This Josephson waveform synthesizer (JWS) allows generation of dc voltages and waveforms by rapidly switching between the different array segments. For example a 50 Hz synthesized stepwise-approximated sine wave is shown in figure 10 with 32 samples per period and 10 V amplitude. The error for the RMS value for such JWS waveforms is directly related to the duration of the transitions between Shapiro steps. During these transients, the array voltage is not quantized and special care has been taken to reduce their duration in the experimental setup.

Coaxial cables with 50 Ω characteristic impedance have been used to connect the bias electronics to the array segments

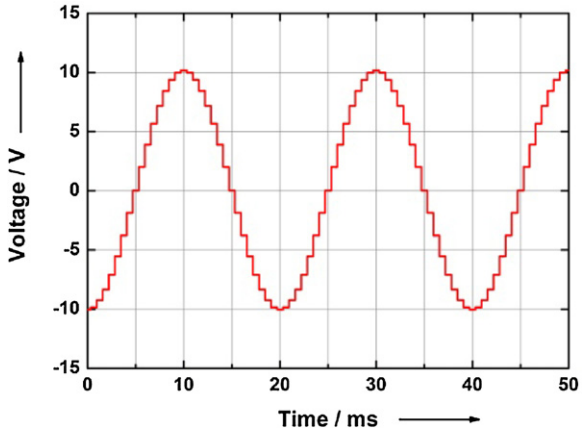

Figure 10. 50 Hz stepwise-approximated Josephson waveform with 32 samples and 10 V amplitude.

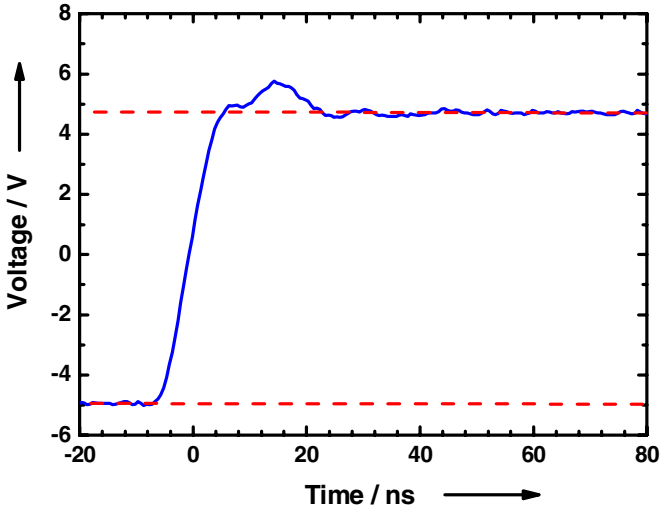

Figure 11. Transient for the largest segment of a 10 V array.

as well as for the output of the array. The 50 Ω resistor in series with the unloaded voltage output reduces the effect of multiple reflections for $V(t)$ at a high impedance load (Williams *et al* 2007). The transients at the JWS output were measured with a fast oscilloscope and are presented in figure 11. The total duration of the edge is clearly shorter than 20 ns and the settling time to the quantized state is less than 100 ns.

4.1. Thermal converter measurements

Initial work was directed towards the determination of the RMS value of these Josephson waveforms. A first experiment using the PJVS by Hamilton *et al* (1995) showed that the uncertainty is limited by the precise knowledge of the transients. For a large number of samples (cf figure 10) the transients usually vary and thus make the calculation of the RMS value difficult. Therefore, fast-reversed dc (FRDC) measurements on planar multi junction thermal converters (PMJTC) have been suggested by Burroughs *et al* (1999b). In these FRDC measurements transients do not play a role because they are introduced in the same way for the ac and FRDC waveforms. The only difficulty in the experiment is

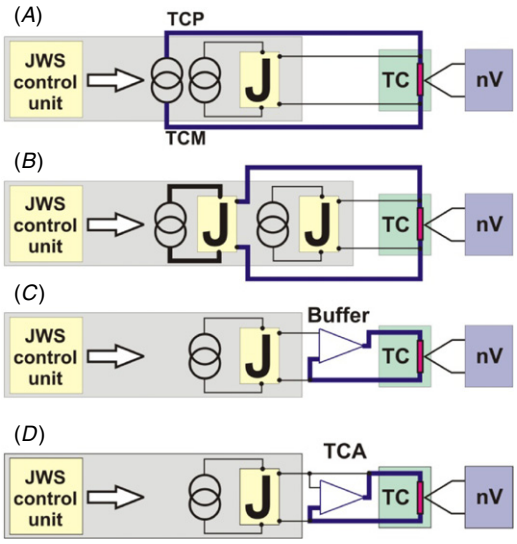

Figure 12. Josephson arrangements to perform ac–dc transfer difference calibrations on thermal converters: (*A*) with additional bias sources, (*B*) with two Josephson systems, (*C*) inserting a buffer amplifier and (*D*) by using a TCA.

to drive the low impedance PMJTC devices, typically in the range from 90 Ω to 1.5 kΩ, without losing quantization by the current involved, see e.g. Behr *et al* (2001). This requires an additional current supply in order to transfer the array voltage on a separate, zero-current connection. Thicker lines show the current carrying connections in the different setups for ac–dc transfer measurements shown in figure 12. In (*A*) and (*B*) the load current is fed to the PMJTC synchronously with the ac voltage and carefully adjusted in amplitude to keep the Josephson array on the required step (cf Behr *et al* (2005) and Djordjevic *et al* (2010), respectively). In (*C*) a buffer amplifier (Budovsky and Hagen 2010, Séron *et al* 2012) drives the current to the PMJTC. Budovsky *et al* (2012) used a transconductance amplifier for this purpose. In spite of the limitation due to the transients it was clear that the error of the RMS values decreases with diminishing frequencies and that the values are more precise with faster transients. A first precision synthesis of Josephson waveforms with uncertainties better than 1 μV V^{-1} was demonstrated for the frequency range below 200 Hz (Behr *et al* 2005). The PMJTC was driven by two additional, synchronized current sources (TCP and TCM in figure 12(*A*)). The JWS is set to produce, at equal time intervals, synthesized ac and positive and negative dc voltages of similar RMS magnitudes in a sequence dc+/ac/dc−. The output voltage of the PMJTC is measured with a nanovoltmeter at every stage of the sequence after a 20 s delay. This delay time has been evaluated as the best compromise between the settling time of the PMJTC and its short-term thermal drift. From the nanovoltmeter readings, the experimental ac–dc transfer difference is the average of the measured PMJTC voltages in the ac mode and the average of the measured voltages in both dc polarities. The ac–dc transfer difference for the PMJTC is then calculated as the difference of the measured minus the theoretical value. The theoretical value is calculated from the Josephson voltages.

The ac–dc transfer difference was measured in the frequency range from 5 Hz to 2 kHz using 250 samples. At

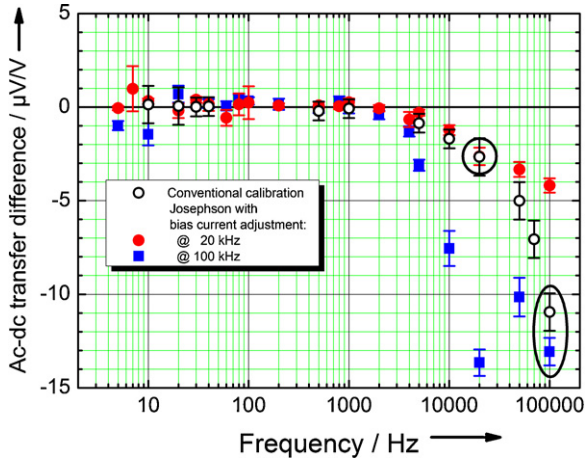

Figure 13. Ac–dc transfer difference calibration of a PMJTC using a 4-sample waveform. The bias current for the Josephson array has been adjusted one time at 20 kHz (red dots) and another time at 100 kHz (blue squares).

low frequencies, an increase of the ac–dc transfer difference for PMJTC appears, which is a characteristic of these devices (Laiz *et al* 2003). The measurements were in good agreement with a calibration of the same PMJTC using sampling methods (Ihlenfeld *et al* 2003).

Towards higher frequencies the expected linear increase with sine wave frequency due to the limited 200 ns rise time of the bias source was observed. The linear increase with frequency was in good agreement with the error calculated for a rise time of 185 ns. This result was encouraging and further improvements were expected. After realizing much faster transients with 5 ns rise time and using special arrangements to suppress reflections (Williams *et al* 2007) settling times were clearly below 100 ns (cf figure 11). However, uncertainties in ac–dc transfer measurements did not improve. Experimental and theoretical efforts have been undertaken to understand the limitations. Experimentally, Djordjevic *et al* (2010) improved the finite resolution of the 14-bit DACs for TCP and TCM by a second JWS (figure 12(*B*)).

In parallel, two papers starting from different physical assumptions came to approximately the same result—the level of quantization for the RMS value of JWS waveforms is limited (Burroughs *et al* 2008, Lee *et al* 2009). It can be expressed e.g. as the slope of a voltage step for every change in bias current trim and signal frequency of typically of 2 μV V^{-1}/(mA kHz) at 1 kHz. This slope depends on the step widths of the zero and first Shapiro steps and thus on many parameters such as microwave frequency and power, which itself depends on the helium level.

However, it has been shown that for transients with overshoot (cf figure 11) an operating point can be found where the overshoot exactly compensates for the losses due to the limited rise time (Eklund *et al* 2011, Séron *et al* 2012). The RMS value at this point corresponds to the ideal RMS value with zero-duration transients. Therefore, approximate knowledge of the ac–dc transfer difference of the PMJTC at a high frequency is sufficient to set the operating point of the JWS without precise knowledge of the transients. In figure 13 a measurement is shown using this method for a 4-sample

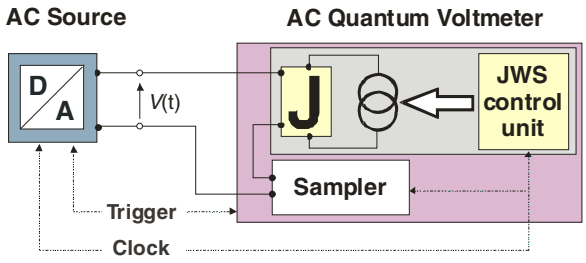

Figure 14. Schematic diagram of the ac quantum voltmeter.

waveform and the setup (*B*) in figure 12. The conventional transfer difference of the PMJTC is shown with the open circles. The bias current of the array is trimmed to roughly match the transfer difference at a high frequency. Even though deviations can be up to 5–6 μV V^{-1} at a frequency of 10 kHz, see the difference between the squares and the dots, due to the linearly improving uncertainty of the Josephson waveform towards lower frequencies, uncertainties are clearly below 1 and 0.1 μV V^{-1} at 1 kHz and 100 Hz, respectively. This way of using additional information, shown as circles in figure 13 and which itself does not need to be very precise, helps performing easy thermal converter calibrations using a buffer amplifier (Séron *et al* 2012) or transconductance amplifier (TCA) (Budovsky *et al* 2012) as shown in figures 12(*C*) and (*D*), respectively. Although the stepwise-approximated waveforms do not lead to a true quantum standard due to the transients involved, the system achieves uncertainty values of better than 1 μV V^{-1} for frequencies from a few Hz up to 1 kHz. In the future this way of unloading the Josephson array may have a high potential for industrial applications.

4.2. Ac quantum voltmeter

As discussed in section 4.1, transients limit the uncertainty of direct synthesis using binary Josephson arrays. Here we discuss the idea of combining binary Josephson arrays and sampling methods first introduced by Behr *et al* (2007). Sampling voltmeters are broadly employed worldwide and detailed analysis has shown that the gain and reference error of the sampling voltmeter dominates the uncertainty of their measurements (Ihlenfeld 2001). In order to improve the uncertainty, the sampling voltmeter can be used as a null detector between the periodic signal to be calibrated and a JWS waveform synthesized synchronously and in phase, as shown in figure 14. The sampling voltmeter is used in a similar way as null detectors in dc Josephson calibrations and measures the small difference between the periodic signal and the time-varying Josephson reference voltage (cf figure 15). This combination of a sampling voltmeter and a JWS can be used as an 'ac quantum voltmeter' to measure periodic waveforms from an ac source or device under test (DUT) up to audio frequencies. Proper triggering ensures sampling the signal while the JWS is on a quantized step. The voltage measurements are therefore automatically calibrated, and at the same time, the influence of the transients between quantized steps is eliminated. Due to the direct link to the quantum voltage standard and the low voltage measured by the null detector, a significant improvement of the uncertainty is achieved.

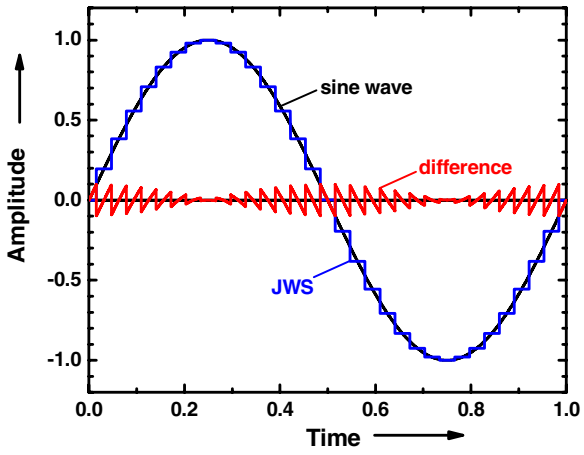

Figure 15. Principle of the differential sampling method.

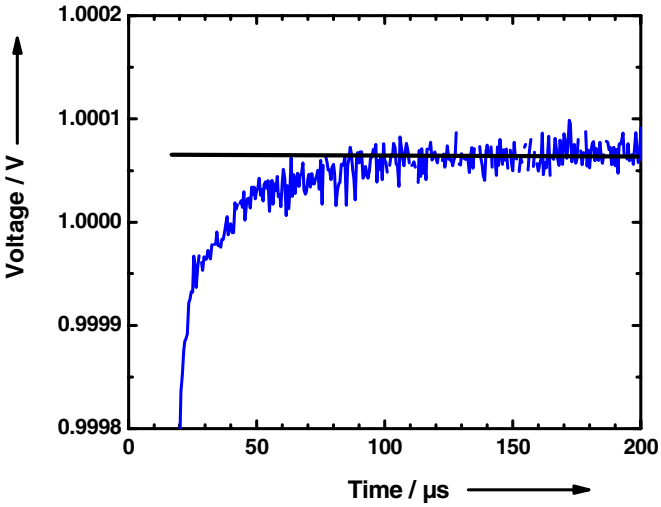

Figure 16. Reading of the sampling voltmeter after a 1 V step jump.

This method was proposed and demonstrated for 4-sample waveforms by Behr *et al* in 2007. However, even though the transients are outside the sampling windows, they influence the settling time of the sampling voltmeter through e.g. charging up the input filter. This limits the maximum integration time besides noise and resolution. Figure 16 depicts a time trace after a voltage jump from 0 to 1 V and clearly demonstrates this limitation. The step was measured with a digital sampling voltmeter in the 1 V range using an integration time of 10 μs. The start of the integration was shifted by 1 μs for each point displayed. Although the transients are shorter than 100 ns (cf figure 11) the voltmeter still indicates a deviation of 10^{-4} from the true voltage after 20 μs and settling is not reached till 60–80 μs. Very similar effects have been seen by others (Ihlenfeld *et al* 2005, Rüfenacht *et al* 2008, van den Brom *et al* 2009).

Nevertheless a comparison at the 10 V level has been made up to kHz-frequencies in order to demonstrate the ac quantum voltmeter principle. Two JWSs have been programmed to generate waveforms with a defined phase relationship. The microwave frequencies and number of junctions biased in each array have been chosen to match the amplitudes to within 100 nV. The initial time delay of the sampling voltmeter is toggled in order to alternate the polarity of the 4-sample sine

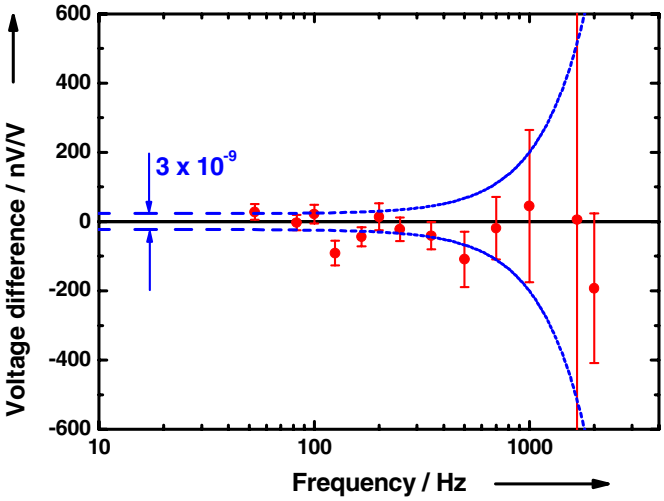

Figure 17. Direct comparison of two 4-sample Josephson waveforms with a sampling voltmeter.

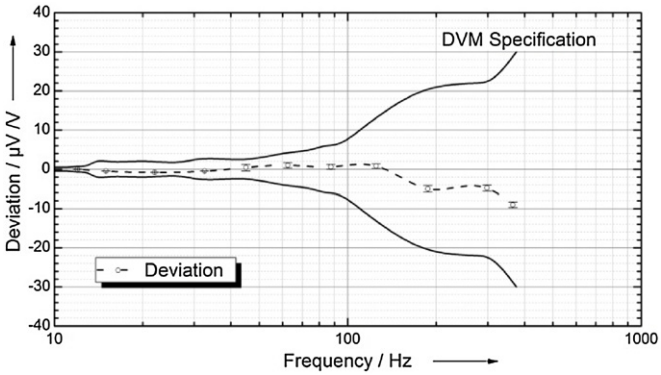

Figure 18. Deviation of the RMS value computed from samples from the true RMS value determined from the amplified quantized steps in the time domain on the 10 V input range of the DVM. The standard deviation of the measurements is very small and not readily apparent.

wave measured. The measurements in figure 17 were taken over 500 polarity reversals, equivalent to a measurement time of about 30 min. Allan variance analysis indicated that the optimal sampling windows contained 128 and 256 waveform periods of the ac signal depending on the integration time used. For every frequency, the integration time has been selected in the range from 10 μs at 2 kHz up to 1 ms at 70 Hz. The difference between these integration times and the much longer duration of each sample in the waveform is due to the settling effects.

The type-A uncertainty of the method is indicated by the dashed line in figure 17, demonstrating an improvement by about two orders of magnitude in comparison to the direct sampling method. At frequencies below 400 Hz, the uncertainty is 3 nV V^{-1}. Towards higher frequencies, the uncertainty increases as the integration time becomes shorter and shorter. Rectangular waveforms have been used up to 6 kHz for impedance calibrations (Lee *et al* 2010). However, for many ac applications it is important to increase the number of samples in each JWS period to better approximate a specific waveform. The time the binary Josephson system stays on a quantized voltage level is therefore reduced, and the accessible frequency range is limited. For a sinewave approximation using many samples, successful measurements have been demonstrated (Rüfenacht *et al* 2008, 2009, 2011, Kim *et al* 2010, Williams *et al* 2011). Due to the large number of samples used, frequencies have been limited to below 100 Hz so far, but very good uncertainties of a few parts in 10^8 at the 1 V level have been achieved.

4.3. Characterization of analogue to digital converters

As shown in equation (2), the output voltage of a Josephson array follows a perfect frequency to voltage relationship. The microwave frequency can easily be locked to ± 1 Hz and referenced to a well-known timebase. Therefore, the array voltage is defined to parts in 10^{11} and is, for practical purposes, free from noise and constant in time. These characteristics make Josephson voltages ideal for the characterization of analogue to digital converters (ADCs). Transferring these characteristics to room temperature requires the use of adequate techniques both for the selection of the cables used, in order to minimize thermal emfs, and on the design of the measurement procedure. Care must also be taken to determine whether the observed drift originates in the measuring instrument itself. The Allan deviation (e.g. Witt 2005) is a very powerful tool to analyse whether the assumptions about the quality of the measurement procedure are still valid for the chosen measurement procedure. For ac waveforms, it allows setting the maximum number of periods that can be processed before drifts in the system, for instance from the semiconductor voltage reference in a voltmeter or the thermal emfs, limit the uncertainty that can be reached.

These noise- and drift-free voltages have been used to measure the linearity of digital voltmeters (DVMs) (Giem 1991). Using a JWS to output the dc voltages required greatly simplifies this procedure (Burroughs *et al* 1999a). Furthermore, the JWS can also be used to dynamically characterize ADCs, used in numerous applications in metrology. ADCs or DVMs normally include a high impedance stage at their input and do not load the JWS. Consequently, the JWS can be connected directly to the DUT without additional synchronized current sources.

The first dynamic Josephson ADC characterization of an $8\frac{1}{2}$-digit, or 28-bit, DVM was reported in Ihlenfeld *et al* (2005). A 1 V JWS followed by an amplifier was used to characterize the 10 V input range of the DVM. Figure 18 shows the uncertainty for the calculation of the RMS value of the signal sampled by the DVM. As the results clearly show, the performance that can be achieved clearly improves the manufacturer specifications.

As a consequence of these results, a project was started to integrate such a DVM calibration into the primary standard for electrical power at PTB, as reported in Palafox *et al* (2007, 2009). In the latest version, a 10 V JWS was used to determine the gain error of the DVM using exactly the same parameters as when sampling the voltage and current waveforms in the power standard. The target uncertainty of 0.4 μV V^{-1} was reached within 100 signal periods, or 1.6 s, as shown in figure 19. Other

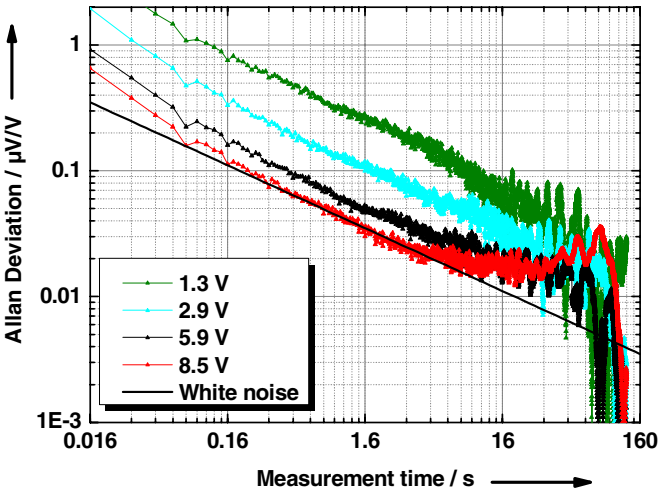

Figure 19. Allan deviation of the gain error for each individual period of a 62.5 Hz signal with different peak amplitudes. A line corresponding to white noise is included as a visual aid. The target uncertainty of 0.4 μV V^{-1} is reached in 1.6 s or 100 periods.

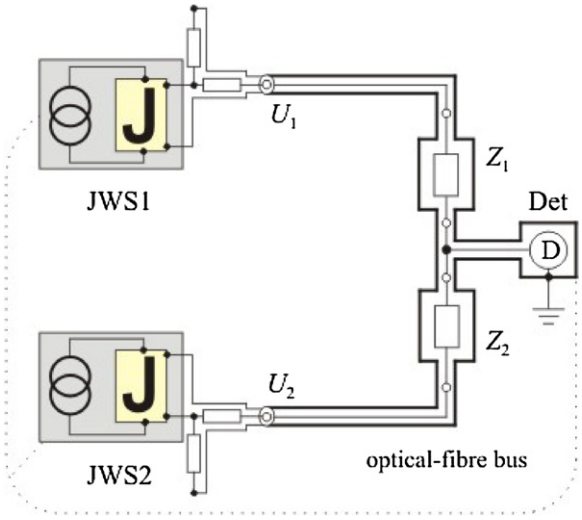

Figure 20. Schematic diagram of a 2TP Josephson impedance bridge. The two 50 Ω resistors at the output of each JWS and the corresponding length of cable to cancel out reflections at the detector are also indicated.

power standards employ the ac quantum voltmeter measuring principle explained in the previous section (Waltrip *et al* 2009, Djokic 2010).

The superior characteristics offered by JWS signals relative to other signal generators have also been exploited to characterize ADCs used or designed for metrological applications (Iuzzolino *et al* 2009, 2011, Overney *et al* 2011, Rietveld *et al* 2011). In between calibrations, the ADC or DVM is effectively used as a transfer standard. Another application of these characterizations is to measure the difference between Josephson waveforms generated using a JWS or a JAWS system. Kohlmann *et al* (2009) report a difference of less than 4 nV, or 0.5 μV V^{-1}, for the comparatively small amplitude of 8 mV used in the frequency range from 50 Hz to 4 kHz. With an amplitude of 104 mV, Jeanneret *et al* (2011) reached a combined uncertainty of 0.26 μV V^{-1} ($k = 2$) at 500 Hz.

4.4. Impedance measurements

Conventional arrays have been used (Warnecke *et al* 1987) to measure the ratio at dc between two resistance standards with an uncertainty of 30 nΩ Ω^{-1} ($k = 1$). An external current source was employed and the JVS was connected as a potentiometer to measure the voltage across each resistor in sequence. The deterministic and quickly adjustable voltages made possible by programmable Josephson arrays allowed a significant reduction in the uncertainty to a few nΩ Ω^{-1} some years later (Behr *et al* 2003). In contrast to these potentiometric measurements, Josephson impedance bridges, shown in figure 20, extend the capability to measure impedances into ac. They use two JWSs to set the current that flows in the impedance bridge. They were introduced in Lee *et al* (2010) as a two terminal pair (2TP) bridge in order to determine the ratio between two impedances over a wide frequency range. The two impedances in the bridge are compared in terms of the amplitudes of the JWSs. These can be adjusted coarsely via the number of JJs biased in each array. The bridge is then balanced by adjusting the

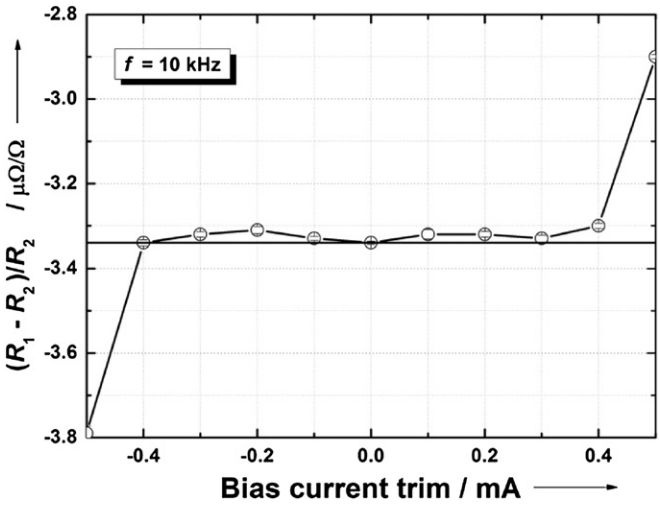

Figure 21. Variation of the in-phase component of the ratio between two 10 kΩ resistors at 10 kHz as a function of bias current trim for one of the Josephson arrays in the bridge.

microwave frequency used in one of the JWS. The phase angle between the two waveforms is adjusted through the synchronization electronics, with a resolution of 1 ps. One of the JWS also generates the reference signal for the detector, where it is optically isolated. As the bias sources are isolated from other electrical potentials, the current flowing through the impedances has to return through the outer conductor, making the 2TP Josephson impedance bridge coaxial.

The influence of variations in transitions between quantum-defined voltages is minimized by using square waves as suggested by Hellistö *et al* (2003). As figure 21 shows, these changes are below the resolution of the measurement setup even at 10 kHz for the ratio between two 10 kΩ resistors. The contribution to the measured ratio due to the 50 Ω resistors in series with the impedances Z_1 and Z_2 is removed by taking the average between *forward*, JWS1 connected to Z_1, and *reverse*,

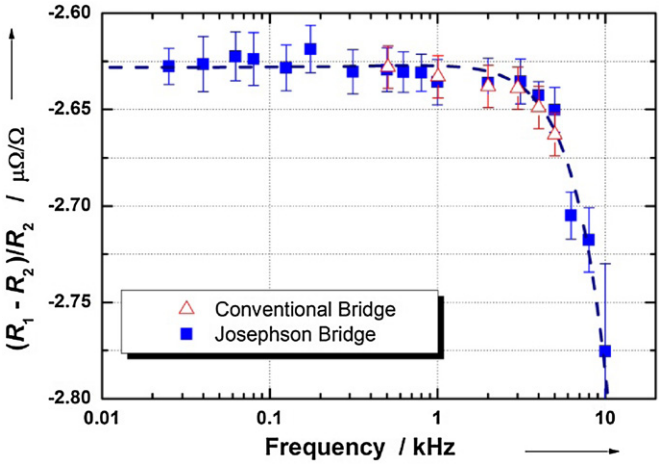

Figure 22. Measured ratio between two 10 kΩ resistors as a function of frequency.

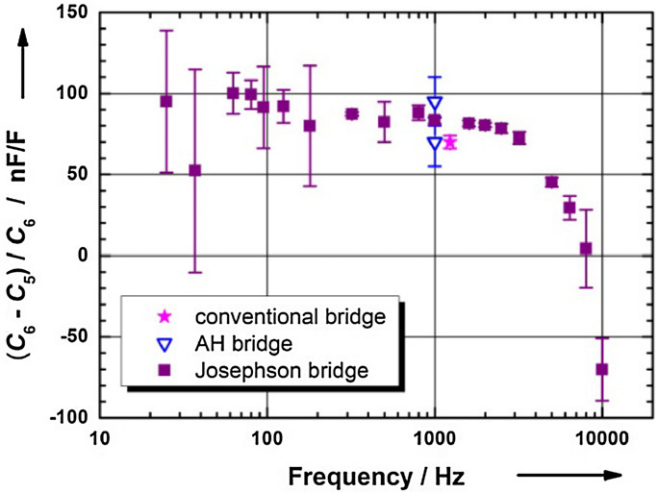

Figure 23. Measured ratio between two 100 pF capacitors as a function of frequency.

JWS1 connected to Z_2, bridge configurations. Figure 21 shows the ratio measured in the *forward* configuration.

Figure 22 shows the measured ratio between two 10 kΩ resistors in a temperature controlled enclosure as a function of signal frequency. The triangles show the results from a conventional manually operated 2TP coaxial bridge with a combined uncertainty of 11 nΩ Ω^{-1} ($k = 1$) in the frequency range between 500 Hz and 10 kHz. The 2TP Josephson impedance bridge results show excellent agreement and comparable uncertainty of 20 nΩ Ω^{-1} ($k = 1$). Moreover, this low uncertainty is available over a much wider frequency range, down to 25 Hz. Each point in figure 22 is the average of four sets of *forward–reverse* measurements. Each individual frequency sweep takes less than 30 min and runs under complete software control. At the moment, the change between *forward* and *reverse* configurations is performed manually.

The applicability of the 2TP Josephson impedance bridge has been extended to the comparison of two 100 pF capacitance standards, as shown in figure 23. Despite the considerable increase in the magnitude of the impedances in the bridge, the results also show very good agreement to 20 nF F^{-1} with measurements from a conventional coaxial bridge at 1233 Hz. Results measured with a commercial bridge are also shown at 1 kHz. The Josephson 2TP results improve the uncertainty at lower frequencies to the level of 0.1 μF F^{-1} (cf Palafox *et al* 2012).

5. Pulse driven Josephson arrays

Although binary Josephson arrays are successfully used for different ac applications, their use is limited because of the transients between different Shapiro steps. As indicated in section 2, pulse driven arrays or the JAWS can also generate quantum accurate waveforms. In this JAWS, a fixed number of JJs is driven by short current pulses. Each pulse transfers n flux quanta Φ_0 through each junction. Using the Josephson array as a quantizer for the input waveform, any desired waveform up to the MHz range can be synthesized. The generated waveforms show spectral purity larger than –115 dBc and the desired spectrum becomes programmable. The pulse pattern can be calculated either for a given spectrum or for time domain signal desired. The output peak-to-peak voltage V_{PP} for a series array of m junctions is given by (cf equation (2))

$$V_{PP}(t) = 2mn\Phi_0 f_{\text{clock-PPG}} A_{\Sigma\Delta}, \tag{4}$$

where $f_{\text{clock-PPG}}$ is the clock frequency of the pulse pattern generator (PPG) and $A_{\Sigma\Delta}$ ($0 < A_{\Sigma\Delta} < 1$), the $\Sigma\Delta$-code amplitude factor. The amplitude factor must be <1 to ensure a stable $\Sigma\Delta$ simulation. A code length $L_{\Sigma\Delta}$ used for $T_{\Sigma\Delta}$ periods result in a signal frequency f_{ac} given by $f_{ac} = (T_{\Sigma\Delta} f_{\text{clock-PPG}})/L_{\Sigma\Delta}$. The maximum length of the pulse pattern limits the lower frequency that can be synthesized. In addition, dc voltages can be generated by sending a pulse pattern that does not change in time. The JAWS principle was first demonstrated by NIST (Benz and Hamilton 1996).

5.1. Design

A basic requirement for operation with pulses is the broadband performance of the arrays over a wide frequency range. The characteristic frequency should therefore be equal to the clock frequency (Benz and Hamilton 1996). Commercially available PPGs suitable for 15 GHz characteristic frequencies are normally used for this application. Furthermore the array designs should enable a homogeneous distribution of the pulse power for the whole array. Then all junctions will reliably transfer flux quanta at a fixed pulse amplitude for all pulse repetition frequencies. The JJs are typically arranged in the centre conductor of a 50 Ω coplanar waveguide, which is terminated by a lumped resistor. In this context, lumped takes the usual high frequency and microwave meaning of being short compared to the characteristic wavelength.

For easy operation with pulses, lumped arrays can be used (cf Benz and Hamilton 1996, Kieler *et al* 2007), but the restriction in length limits the number of junctions that can be integrated and therefore the output voltage. Extended arrays (Benz *et al* 1999) circumvent these limitations. These arrays are considerably longer than the wavelengths corresponding to the relevant frequencies of the current pulses and thus more

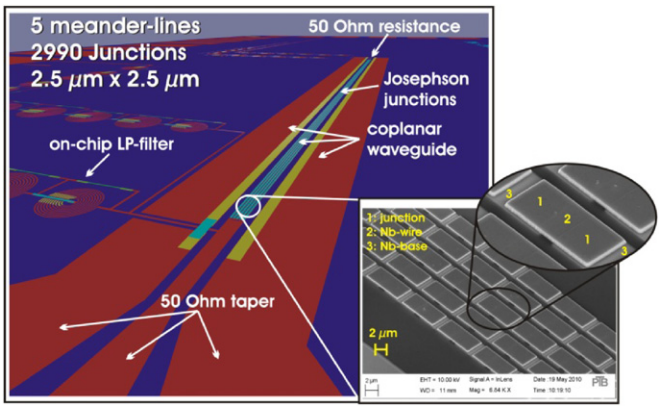

Figure 24. Example of a JAWS chip design made at PTB. The inset shows the SEM pictures of the meander structure in the centre conductor and two JJs.

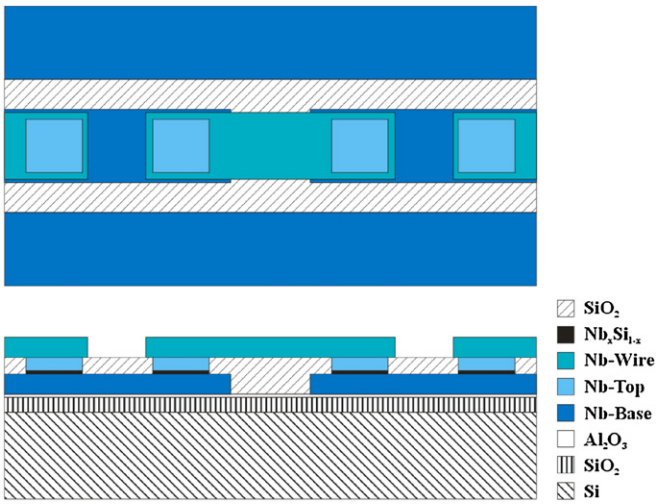

Figure 25. Schematic of four junctions within an SNS series array: top view (top) and cross section (bottom).

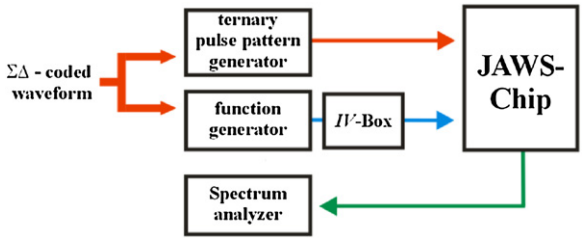

Figure 26. Schematic of the experimental JAWS setup used at PTB. The synchronization signals are not included for clarity.

junctions can be integrated. To avoid errors due to the common mode voltage caused by the 50 Ω termination, the pulses can be ac coupled (Benz *et al* 2001). For this coupling technique an additional low frequency compensation signal has to be applied.

Specially designed on-chip low-pass filters are arranged at the low frequency output leads and the connections for the compensation signal to restrict the propagation of the input pulses along the coplanar line (cf Chevtchenko *et al* 2005, Watanabe *et al* 2006). Figure 24 shows a design picture of an extended array where the junctions are arranged in meander-lines (Kieler *et al* 2007). The filters can be seen on the left and the insets show scanning electron microscope (SEM) pictures of the JJs in the meander-lines.

5.2. Fabrication

The JAWS is based on overdamped junctions, which have predominately been realized by SNS junctions. Different materials have been used for the barrier as e.g. PdAu (Benz *et al* 2001), HfTi (Hagedorn *et al* 2006) or Nb_xSi_{1-x} (Baek *et al* 2006). The resistivity of the barrier material should be rather high in order to realize suitable characteristic frequencies around 15 GHz.

At PTB, we used SNS junctions based on $Hf_{wt\%50}Ti_{wt\%50}$ as the normal metal. These junctions have a high critical current density of about 60–80 kA cm^{-2}, which is adjusted by the thickness of the barrier layer. This has the advantage that many sub-μm junctions can be integrated in lumped arrays. The resulting high normal state resistance results in significant heat generation in large arrays and eventually leads to the suppression of the superconductive state. Therefore, the critical current has to be small and consequently the characteristic frequency $f_c = 5$ GHz is small as well as the width of the Shapiro step. The operating margins for pulse drive then become rather small. To increase the characteristic frequency f_c without increasing the critical current density j_c, at PTB we changed the barrier material to Nb_xSi_{1-x} (cf section 3). A characteristic frequency of $f_c = 15$ GHz can be adjusted, keeping j_c at moderate values of about 20–30 kA cm^{-2}.

Figure 25 schematically shows the top view and cross section of a series SNS array. The fabrication process was developed for large arrays of small JJs (Hagedorn *et al* 2006). To ensure a low parameter spread of the junction dimensions Al-hard masks are used instead of photoresist. The small size of the junctions prevents using a window-type process. Chemical mechanical polishing (CMP) is applied to 'open' a contact surface to the Nb-top electrode. The Nb-wiring layer connecting JJs is deposited on top of an absolutely flat surface and therefore achieves the maximum superconductive current possible. E-beam lithography is used to ensure a high alignment precision and to provide contact-free lithography. Large arrays of sub-μm junctions (down to 0.04 μm^2 junction area) with high yield can be fabricated by the combination of CMP and e-beam lithography.

5.3. Measurements and applications

Figure 26 shows the simplified schematic of the experimental setup used to generate spectrally pure and arbitrary waveforms at PTB.

The desired waveform is encoded by a ΣΔ modulation into a series of 0/1/–1 pulses (Kieler *et al* 2009). This bit pattern is transferred into the memory of the PPG. The PPG (Sympuls BPG 30G-TER[3], cf van den Brom *et al* (2008))

[3] Commercial instruments are identified in this paper in order to adequately specify the experimental procedure. Such identification does not imply recommendation or endorsement by PTB.

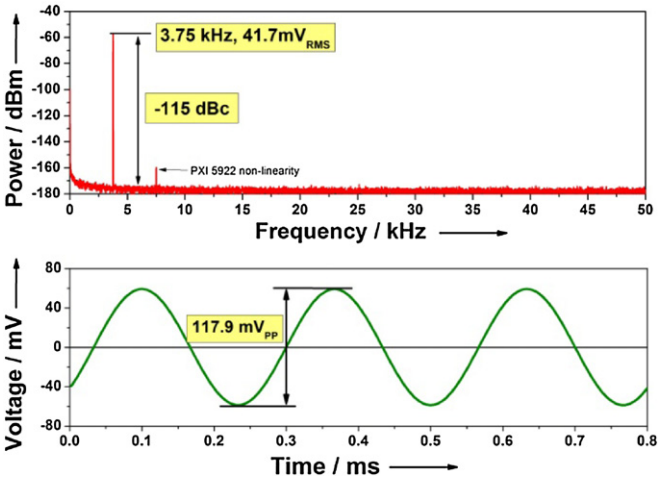

Figure 27. Frequency spectrum and time domain trace of a synthesized sinusoidal waveform ($f = 3.75$ kHz, $V_{PP} = 117.9$ mV, $m = 2000$ JJs, $f_{clock\text{-}PPG} = 15$ GHz, $A_{\Sigma\Delta} = 0.95$).

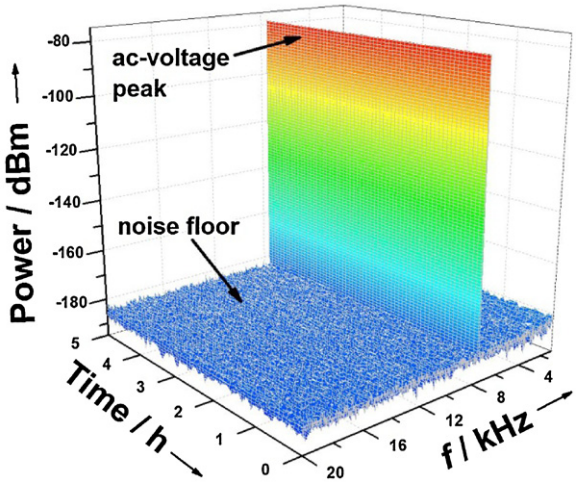

Figure 28. Time stability of a synthesized sinusoidal waveform ($f = 7.5$ kHz, $V_{PP} = 11.1$ mV, $m = 2990$ JJs, $f_{clock\text{-}PPG} = 3$ GHz, $A_{\Sigma\Delta} = 0.90$).

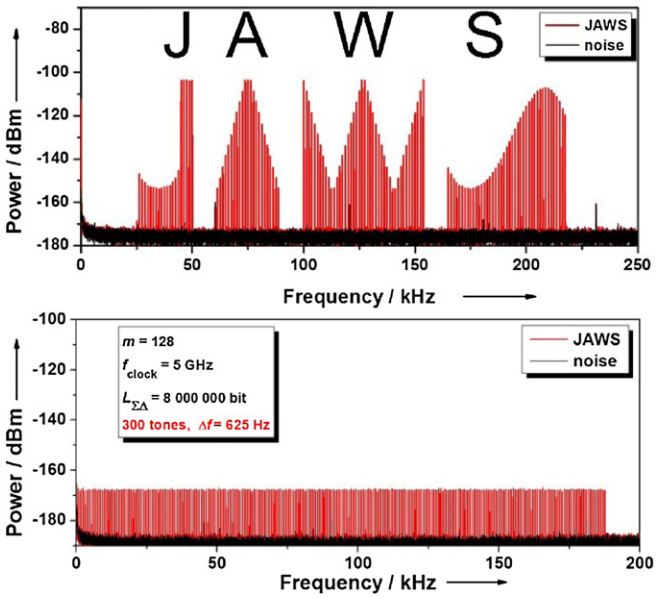

Figure 29. Examples for arbitrary waveforms: 'JAWS' waveform (top), 300 tone comb waveform (bottom).

delivers bipolar current pulses, which are transmitted to the JAWS chip operated at 4.2 K. The compensation signal is provided by the function generator. A spectrum analyser is used in order to analyse the synthesized waveform. Quantized operation is realized by adjusting the amplitudes of the pulses and of the compensation signal and can be identified by the complete suppression of the unwanted harmonics in the frequency spectrum.

Figure 27 shows a typical frequency spectrum and the corresponding time domain trace of a synthesized sinusoidal waveform with a frequency of 3.75 kHz and a peak-to-peak voltage of about 117.9 mV. A series array of 2000 NbSi SNS junctions was used to generate this signal with a clock frequency of 15 GHz. The noise floor of the digitizer is at about –180 dBm and all higher harmonics have smaller amplitudes. Consequently the signal-to-noise ratio is –115 dBc which is excellent. The remaining tone at 7.5 kHz is a nonlinearity of the ADC used (cf Benz *et al* 2007).

To check the precision of the JAWS we performed an indirect calibration using the ac-PJVS (see section 4) to calibrate the ADC used (NI-PXI 5922, see footnote 3). The time stability of synthesized waveforms is an essential requirement for JAWS applications. Figure 28 demonstrates the very high stability in time of a sinusoidal waveform synthesized with a series array of 2990 HfTi SNS junctions. The spectrum remained unchanged over five hours without any readjustment of the operating parameters in the JAWS setup.

To demonstrate the capability of the JAWS system to generate arbitrary waveforms figure 29 shows the frequency spectrum of two special waveforms. First, the acronym 'JAWS' was reproduced with 131 tones in the frequency range from 25 kHz to about 220 kHz ($m = 128$ JJs). The lower waveform shows a frequency comb of 300 tones up to about 190 kHz. Each tone is separated 625 Hz from one another. The last waveform is suitable for applications in metrology such as the characterization of electronic devices as shown for a broadband amplifier (Kieler *et al* 2010, Henderson *et al* 2008). Figure 30 displays the frequency spectrum at the output of the amplifier.

The amplifier does not add any harmonics to the JAWS signal and raises the amplitude to 441 mV RMS. The noise floor increased to values of about –140 dBm, but the signal-to-noise ratio is still –100 dBc. The frequency response of this amplifier was determined using different waveforms (single tone and frequency combs cf figure 29 bottom) and different detection devices (thermal converter and fast ADC). The –3 dB frequency of the amplifier is outside of the shown frequency range. At the frequency of 1 kHz we determined an amplifier gain of 100.90 ± 0.05.

Other applications are ac–dc thermal converter measurements (Schleussner *et al* 2010, Kieler *et al* 2008, van den Brom and Houtzager 2010). A low voltage version of the JAWS providing a pseudo-random noise waveform is used for Johnson noise thermometry and an 'electrical' measurement

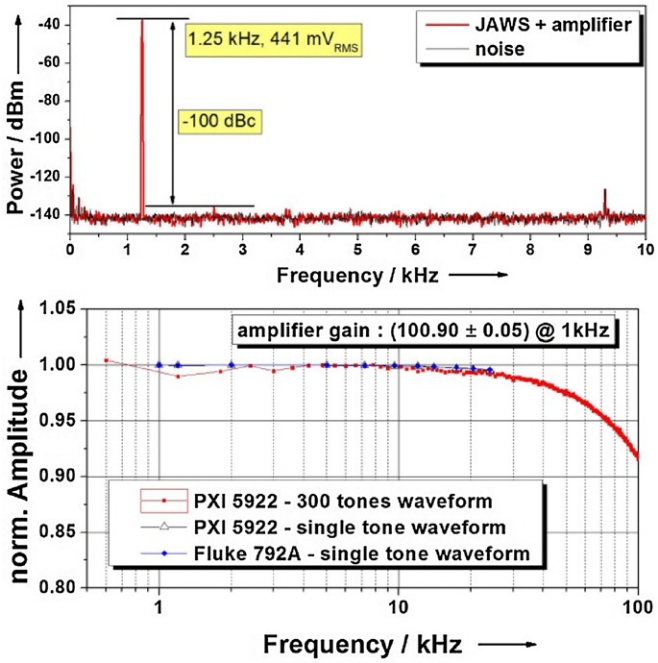

Figure 30. Frequency spectrum at the output of the amplifier (top) and measured gain as a function of frequency (bottom).

of Boltzmann's constant (Benz *et al* 2009b, 2011). Another application is the characterization of fast ADCs (e.g. Toonen and Benz 2009, Iuzzolino 2011).

These examples clearly demonstrate that, despite the rather small voltages of JAWS systems, promising results have been achieved. The big challenge for the future still is the increase of the output amplitude to at least 1 V.

6. Conclusions

Just over a century after the discovery of superconductivity and nearly 50 years after the discovery of the Josephson effects, electrical metrology and high-precision voltage measurements can no longer be imagined without series arrays of JJs. We have briefly summarized the main contributions from PTB as part of the worldwide effort that led to the establishment of JVSs for the representation of the voltage unit in 1990. Conventional 10 V JVSs are well established at some 50 NMI and calibration laboratories for dc measurements and are commercially available.

The development of programmable Josephson series arrays voltage standards opened up the world of ac applications and became the next chapter in this exciting story about applications of the Josephson effect in metrology. The ideas and the significant progress in fabrication technology presented in section 3 have enabled routine fabrication of binary 1 and 10 V arrays. In this paper, we have also presented PTB's pioneering applications using these arrays for the ac quantum voltmeter, for dc resistance metrology and in Josephson impedance bridges. Other metrological applications of Josephson series arrays reviewed in this paper are: automated dc calibrations, calibration of thermal converters, ADCs and of electronic modules. A further application, primary standards for electrical power, exploits Josephson waveforms either for the *in situ* calibration of the voltmeter used or as part of a dual channel ac quantum voltmeter.

The synthesis of completely quantum-defined ac voltages with pulse driven arrays has led to very promising results. We have generated spectrally pure waveforms with higher harmonics suppressed by about 115 dBc. However, the aim to generate 1 V ac voltages is very challenging due to the complex operation using short current pulses.

The applications included in this paper are just a showcase for the possibilities that have become achievable. Other exciting uses lie ahead on the road to quantum-based ac metrology. In the future, conventional JVSs will be replaced more and more by these PJVSs, as they are easier to operate and provide attractive additional possibilities and applications.

Acknowledgments

The authors would like to thank Veit Bürkel, Peter Duda, Bert Egeling, Rolf Harke, Peter Hinze, Guilherme Ihlenfeld, Jinni Lee, Enrico Mohns, Thomas Scheller, Detlef Schleußner, Jürgen Schurr, Thomas Weimann and Rüdiger Wendisch, and other colleagues from PTB who have contributed to the work reviewed in this paper. They would also like to thank Sam Benz and the complete Josephson team at NIST, Ilya Budovsky (NMIA), Alexander Katkov (VNIIM), Bryan Kibble, and Jaani Nissilä (MIKES). The work within this EURAMET joint research project leading to these results was supported in part by the European Community's Seventh Framework Programme, ERA-NET Plus, under Grant Agreement 217257 (JoSy project).

References

Anders S *et al* 2010 European roadmap on superconductive electronics—status and perspectives *Physica* C **470** 2079–126

Baek B, Dresselhaus P D and Benz S P 2006 Co-sputtered amorphous Nb_xSi_{1-x} barriers for Josephson-junction circuits *IEEE Trans. Appl. Supercond.* **16** 1966–70

Bardeen J, Cooper L N and Schrieffer J R 1957 Theory of superconductivity *Phys. Rev.* **108** 1175–204

Barone A and Paternò G 1982 *Physics and Applications of the Josephson Effect* (New York: Wiley)

Barrera A S and Beasley M R 1987 High-resistance SNS sandwich-type Josephson junctions *IEEE Trans. Magn.* **23** 866–8

Behr R, Funck T, Schumacher B and Warnecke P 2003 Measuring resistance standards in terms of the quantized Hall resistance with a dual Josephson voltage standard using SINIS Josephson arrays *IEEE Trans. Instrum. Meas.* **52** 521–3

Behr R, Grimm L, Funck T, Kohlmann J, Schulze H, Müller F, Schumacher B, Warnecke P and Niemeyer J 2001 Application of Josephson series arrays for a dc quantum voltmeter *IEEE Trans. Instrum. Meas.* **50** 185–7

Behr R, Müller F and Kohlmann J 2002 Josephson junction arrays for voltage standards *Studies of Josephson Junction Arrays II: Studies of High Temperature Superconductors* vol 40 ed A V Narlikar (Hauppauge, NY: Nova) pp 155–84

Behr R, Palafox L, Ramm G, Moser H and Melcher J 2007 Direct comparison of Josephson waveforms using an AC quantum voltmeter *IEEE Trans. Instrum. Meas.* **56** 235–8

Behr R, Schulze H, Müller F, Kohlmann J, Krasnopolin I and Niemeyer J 1999 Microwave coupling of SINIS junctions in a programmable Josephson voltage standard *Conf. Digest ISEC'99* pp 128–30

Behr R, Williams J M, Patel P, Janssen T J B M, Funck T and Klonz M 2005 Synthesis of precision waveforms using a SINIS Josephson junction array *IEEE Trans. Instrum. Meas.* **54** 612–5

Benz S P 1995 Superconductor–normal–superconductor junctions for programmable voltage standards *Appl. Phys. Lett.* **67** 2714–6

Benz S P, Burroughs C J and Dresselhaus P D 1999 Operating conditions for a pulse-quantized AC and DC bipolar voltage *IEEE Trans. Appl. Supercond.* **9** 3306–9

Benz S P, Burroughs C J and Dresselhaus P D 2001 AC coupling technique for Josephson waveform synthesis *IEEE Trans. Appl. Supercond.* **11** 612–6

Benz S P, Dresselhaus P D and Burroughs C J 2011 Multitone waveform synthesis with a quantum voltage noise source *Trans. Appl. Supercond.* **21** 681–6

Benz S P, Dresselhaus P D, Burroughs C J and Bergren N F 2007 Precision measurements using a 300 mV Josephson arbitrary waveform synthesizer *IEEE Trans. Appl. Supercond.* **17** 864–9

Benz S P, Dresselhaus P D, Rüfenacht A, Bergren N F, Kinard J R and Landim R P 2009a Progress toward a 1 V pulse-driven AC Josephson voltage standard *IEEE Trans. Instrum. Meas.* **58** 838–43

Benz S P and Hamilton C A 1996 A pulse-driven programmable Josephson voltage standard *Appl. Phys. Lett.* **68** 3171–3

Benz S P and Hamilton C A 2004 Application of the Josephson effect to voltage metrology *Proc. IEEE* **92** 1617–29

Benz S P, Hamilton C A, Burroughs C J, Harvey T E and Christian L A 1997 Stable 1-volt programmable voltage standard *Appl. Phys. Lett.* **71** 1866–8

Benz S P, Qu J, Rogalla H, White D R, Dresselhaus P D, Tew W L and Nam S W 2009b Improvements in the NIST Johnson noise thermometry system *IEEE Trans. Instrum. Meas.* **58** 884–90

Budovsky I, Behr R, Palafox L, Djordjevic S and Hagen T 2012 Technique for the calibration of thermal voltage converters using a Josephson waveform synthesizer and a transconductance amplifier *Meas. Sci. Technol.* **23** 124005

Budovsky I and Hagen T 2010 A precision buffer amplifier for low-frequency metrology applications *Conf. Digest CPEM 2010* pp 28–9

Burroughs C J, Benz S P, Hamilton C A and Harvey T E 1999a Programmable 1 V dc voltage standard *IEEE Trans. Instrum. Meas.* **48** 279–81

Burroughs C J, Benz S P, Hamilton C A, Harvey T E, Kinard J R, Lipe T E and Sasaki H 1999b Thermoelectric transfer difference of thermal converters measured with a Josephson source *IEEE Trans. Instrum. Meas.* **48** 282–4

Burroughs C J, Rüfenacht A, Benz S P, Dresselhaus P D, Waltrip B D and Nelson T L 2008 Error and transient analysis of stepwise-approximated sine waves generated by programmable Josephson voltage standards *IEEE Trans. Instrum. Meas.* **57** 1322–9

Chevtchenko O A *et al* 2005 Realisation of a quantum standard for AC voltage: overview of a European research project *IEEE Trans. Instrum. Meas.* **54** 628–31

Clarke J 1968 Experimental comparison of the Josephson voltage–frequency relation in different superconductors *Phys. Rev. Lett.* **21** 1566–9

Djokic B 2010 Progress in the development of low-frequency quantum-based AC power standard at NRC Canada *Conf. Digest CPEM 2010* pp 233–4

Djordjevic S, Séron O, Behr R and Palafox L 2010 Double Josephson waveform synthesizer for high precision ac–dc transfer measurements *Conf. Digest CPEM 2010* pp 149–50

Dresselhaus P D, Elsbury M, Olaya D, Burroughs C J and Benz S P 2011 10 V programmable Josephson voltage standard circuits using NbSi-barrier junctions *IEEE Trans. Appl. Supercond.* **21** 693–6

Eklund G, Bergsten T, Tarasso V and Rydler K-E 2011 Determination of transition error corrections for low frequency stepwise-approximated Josephson sine waves *IEEE Trans. Instrum. Meas.* **60** 2399–403

Endo T, Koyanagi M and Nakamura A 1983 High-accuracy Josephson potentiometer *IEEE Trans. Instrum. Meas.* **32** 267–71

Giem J I 1991 Sub-ppm linearity testing of a DMM using a Josephson junction array *IEEE Trans. Instrum. Meas.* **40** 329–32

Gurvitch M, Washington M A, Huggins H A and Rowell J M 1983a Preparation and properties of Nb Josephson junctions with thin Al layers *IEEE Trans. Magn.* **19** 791–4

Gurvitch M, Washington M A and Huggins H A 1983b High quality refractory Josephson tunnel junctions utilizing thin aluminium layers *Appl. Phys. Lett.* **42** 472–4

Hagedorn D, Kieler O, Dolata R, Behr R, Müller F, Kohlmann J and Niemeyer J 2006 Modified fabrication of planar sub-μm superconductor–normal metal–superconductor Josephson junctions for use in a Josephson arbitrary waveform synthesizer *Supercond. Sci. Technol.* **19** 294–8

Hamilton C A 2000 Josephson voltage standards *Rev. Sci. Instrum.* **71** 3611–23

Hamilton C A, Burroughs C J and Kautz R L 1995 Josephson D/A converter with fundamental accuracy *IEEE Trans. Instrum. Meas.* **44** 223–5

Hamilton C A, Kautz R L, Stieg M, Chie K, Avrin W F and Simmonds M B 1991 A 24 GHz Josephson array voltage standard *IEEE Trans. Instrum. Meas.* **40** 301–4

Harris R E and Niemeyer J (eds) 2011 Quantum metrology *100 Years of Superconductivity* ed H Rogalla and P Kes (Boca Raton, FL: Taylor and Francis) pp 515–57

Hellistö P, Nissilä J, Ojasalo K, Penttilä J S and Seppä H 2003 AC voltage standard based on a programmable SIS array *IEEE Trans. Instrum. Meas.* **52** 533–7

Henderson D M, Marshall K M, Williams J M, Pickering J and Patel P D 2008 A voltage source for low frequency ac waveforms with quantum traceability to a Josephson array reference using sampling and feedback *Conf. Digest CPEM 2008* pp 76–7

Ihlenfeld W G K 2001 Maintenance and traceability of AC voltages by synchronous digital synthesis and sampling *PTB Report* E-75, Braunschweig, Germany

Ihlenfeld W G K, Mohns E, Bachmair H, Ramm G and Moser H 2003 Evaluation of the synchronous generation and sampling technique *IEEE Trans. Instrum. Meas.* **52** 371–4

Ihlenfeld W G K, Mohns E, Behr R, Williams J, Patel P, Ramm G and Bachmair H 2005 Characterization of a high resolution analog-to-digital converter with a Josephson AC voltage source *IEEE Trans. Instrum. Meas.* **54** 649–52

Iuzzolino R, Palafox L, Ihlenfeld W G K, Mohns E and Brendel C 2009 Design and characterization of a sampling system based on a Σ-Δ analog-to-digital converters for electrical metrology *IEEE Trans. Instrum. Meas.* **58** 786–90

Iuzzolino R J 2011 Josephson waveforms characterization of a sigma-delta analog-to-digital converter for data acquisition in metrology *PhD thesis* Technical University, Braunschweig, Germany

Jain A K, Lukens J E and Tsai J S 1987 Test for relativistic gravitational effects on charged particles *Phys. Rev. Lett.* **58** 1165–8

Jeanneret B and Benz S P 2009 Applications of the Josephson effect in electrical metrology *Eur. Phys. J. Spec. Top.* **172** 181–206

Jeanneret B, Rüfenacht A, Overney F, van den Brom H and Houtzager E 2011 High precision comparison between a

programmable and a pulse-driven Josephson voltage standard *Metrologia* **48** 311–6
Josephson B D 1962 Possible new effects in superconductive tunnelling *Phys. Lett.* **1** 251–3
Josephson B D 1965 Supercurrents through barriers *Adv. Phys.* **14** 419–51
Kadin A M 1999 *Introduction to Superconducting Circuits* (New York: Wiley)
Kautz R L 1992 Design and operation of series-array Josephson voltage standards *Metrology at the Frontiers of Physics and Technology* ed L Crovini and T J Quinn (Amsterdam: North-Holland) pp 259–96
Kautz R L 1995 Shapiro steps in large-area metallic-barrier Josephson junctions *J. Appl. Phys.* **78** 5811–9
Kautz R L 1996 Noise, chaos, and the Josephson voltage standard *Rep. Prog. Phys.* **59** 935–92
Kieler O F, Iuzzolino R and Kohlmann J 2009 Sub-μm SNS Josephson junction arrays for the Josephson arbitrary waveform synthesizer *IEEE Trans. Appl. Supercond.* **19** 230–3
Kieler O F, Kohlmann J and Müller F 2007 Improved design of SNS Josephson junction series arrays for an ac Josephson voltage standard *Supercond. Sci. Technol.* **20** 318–22
Kieler O F, Landim R P, Benz S P, Dresselhaus P D and Burroughs C J 2008 AC–DC transfer standard measurements and generalized compensation with the AC Josephson voltage standard *IEEE Trans. Instrum. Meas.* **57** 791–6
Kieler O F, Schleussner D, Kohlmann J and Behr R 2010 Josephson arbitrary waveform synthesizer for analysis of AC components *Conf. Digest CPEM 2010* pp 157–8
Kim K-T, Kim S-T, Chong Y and Niemeyer J 2006 Simulations of collective synchronization in Josephson junction arrays *Appl. Phys. Lett.* **88** 062501
Kim M-S, Kim K-T, Kim W-S, Chong Y and Kwon S-W 2010 Analog-to-digital conversion for low-frequency waveforms based on the Josephson voltage standard *Meas. Sci. Technol.* **21** 115102
Kohlmann J and Behr R 2011 Development of Josephson voltage standards *Superconductivity—Theory and Applications* ed A M Luiz (Rijeka: InTech) pp 239–60 www.intechopen.com/articles/show/title/development-of-josephson-voltage-standards
Kohlmann J, Behr R and Funck T 2003 Josephson voltage standards *Meas. Sci. Technol.* **14** 1216–28
Kohlmann J, Kieler O F, Iuzzolino R, Lee J, Behr R, Egeling B and Müller F 2009 Development and investigation of SNS Josephson arrays for the Josephson arbitrary waveform synthesizer *IEEE Trans. Instrum. Meas.* **58** 797–802
Kohlmann J, Müller F, Behr R, Hagedorn D, Kieler O, Palafox L and Niemeyer J 2006 Development of Josephson junction series arrays for synthesis of AC voltages and arbitrary waveforms *J. Phys.: Conf. Ser.* **43** 1385–8
Laiz H, Klonz M, Kessler E, Kampik M and Lapuh R 2003 Low-frequency ac–dc voltage transfer standards with new high-sensitivity and low-power-coefficient thin-film multijunction thermal converter *IEEE Trans. Instrum. Meas.* **52** 350–4
Lee J, Behr R, Katkov A S and Palafox L 2009 Modeling and measuring error contributions in stepwise synthesized sine waves *IEEE Trans. Instrum. Meas.* **58** 803–8
Lee J, Schurr J, Nissilä J, Palafox L and Behr R 2010 The Josephson two-terminal-pair impedance bridge *Metrologia* **47** 453–9
Levinsen M T, Chiao R Y, Feldman M J and Tucker B A 1977 An inverse ac Josephson effect voltage standard *Appl. Phys. Lett.* **31** 776–8
Likharev K K 1986 *Dynamics of Josephson Junctions and Circuits* (New York: Gordon and Breach Science)
Lloyd F, Hamilton C A, Beall J, Go D, Ono R H and Harris R E 1987 A Josephson array voltage standard at 10 V *IEEE Electron Device Lett.* **8** 449–50
Maggi S 1995 RF-induced steps in a pulse driven Josephson junction *Inst. Phys. Conf. Ser.* **148** 1243–6
McCumber D E 1968 Effect of ac impedance on dc voltage–current characteristics of superconductor weak-link junctions *J. Appl. Phys.* **39** 3113–8
McDonald D G 2001 The Nobel laureate versus the graduate student *Physics Today* **54** 46–51
Monaco R 1990 Enhanced ac Josephson effect *J. Appl. Phys.* **68** 679–87
Mueller F, Behr R, Weimann T, Palafox L, Olaya D, Dresselhaus P D and Benz S P 2009 1 V and 10 V SNS programmable voltage standards for 70 GHz *IEEE Trans. Appl. Supercond.* **19** 981–6
Müller F, Behr R, Palafox L, Kohlmann J, Wendisch R and Krasnopolin I 2007 Improved 10 V SINIS series arrays for applications in AC voltage metrology *IEEE Trans. Appl. Supercond.* **17** 649–52
Müller F, Köhler H-J, Weber P, Blüthner K and Meyer H-G 1990 A 1-V series-array Josephson voltage standard operated at 35 GHz *J. Appl. Phys.* **68** 4700–2
Müller F, Kohlmann J, Hebrank F X, Weimann T, Wolf H and Niemeyer J 1995 Performance of Josephson array systems related to fabrication techniques and design *IEEE Trans. Appl. Supercond.* **5** 2903–6
Müller F, Pöpel R, Kohlmann J, Niemeyer J, Meier W, Weimann T, Grimm L, Dünschede F-W and Gutmann P 1997 Optimized 1 V and 10 V Josephson series arrays *IEEE Trans. Instrum. Meas.* **46** 229–32
Müller F, Schulze H, Behr R, Kohlmann J and Niemeyer J 2001 The Nb–Al technology at PTB—a common base for different types of Josephson voltage standards *Physica* C **354** 66–70
Niemeyer J 1989 Josephson series array potentiometer *Superconducting Quantum Electronics* ed V Kose (Berlin: Springer) pp 228–54
Niemeyer J, Hinken J H and Kautz R L 1984 Microwave-induced constant-voltage steps at one volt from a series array of Josephson junctions *Appl. Phys. Lett.* **45** 478–80
Overney F, Rüfenacht A, Braun J-P and Jeanneret B 2011 Characterization of metrological grade analog-to-digital converters using a programmable Josephson voltage standard *IEEE Trans. Instrum. Meas.* **60** 2172–7
Palafox L, Behr R, Ihlenfeld W G K, Müller F, Mohns E, Seckelmann M and Ahlers F 2009 The Josephson-effect-based primary AC power standard at the PTB: a progress report *IEEE Trans. Instrum. Meas.* **58** 1049–53
Palafox L, Behr R, Nissilä J, Schurr J and Kibble B P 2012 Josephson impedance bridges as universal impedance comparators *Proc. CPEM 2012 (Washington, DC, USA, 2–6 July)* pp 464–5
Palafox L, Ramm G, Behr R, Ihlenfeld W G K, Müller and Moser H 2007 Primary AC power standard based on programmable Josephson junction arrays *IEEE Trans. Instrum. Meas.* **56** 534–7
Patel P, Williams J M and Janssen T J B M A 2001 A programmable bias source for binary Josephson junction arrays *BEMC 2001 (6–8 November 2001, Harrogate UK)* www.npl.co.uk/publications/a-programmable-bias-source-for-binary-josephson-junction-arrays
Pöpel R 1992 The Josephson effect and voltage standards *Metrologia* **29** 153–74
Pöpel R, Niemeyer J, Fromknecht R, Meier W and Grimm L 1990 1- and 10-V series array Josephson voltage standards in $Nb/Al_2O_3/Nb$ technology *J. Appl. Phys.* **68** 4294–303
Quinn T J 1989 News from the BIPM *Metrologia* **26** 69–74
Rietveld G, Zhao D, Kramer C, Houtzager E, Kristensen O, de Leffe C and Lippert T 2011 Characterization of a wideband

digitzer for power measurements up to 1 MHz *IEEE Trans. Instrum. Meas.* **60** 2195–201
Rogalla H 1998 Josephson junctions *Handbook of Applied Superconductivity* ed B Seeber (Bristol: Institute of Physics Publishing) pp 1759–75
Rüfenacht A, Burroughs C J and Benz S P 2008 Precision sampling measurements using ac programmable Josephson voltage standards *Rev. Sci. Instrum.* **79** 044704
Rüfenacht A, Burroughs C J, Benz S P, Dresselhaus P D, Waltrip B C and Nelson T L 2009 Precision differential sampling measurement of low-frequency synthesized sine waves with an AC programmable Josephson voltage standard *IEEE Trans. Instrum. Meas.* **58** 809–15
Rüfenacht A, Overney F, Mortara A and Jeanneret B 2011 Thermal transfer standard validation of the Josephson-voltage-standard-locked sine-wave synthesizer *IEEE Trans. Instrum. Meas.* **60** 2372–7
Schleussner D, Kieler O F, Behr R, Kohlmann J and Funck T 2010 Investigations using an improved Josephson arbitrary waveform synthesizer system *Conf. Digest CPEM 2010* pp 176–7
Schulze H, Behr R, Kohlmann J and Niemeyer J 2000 Design and fabrication of 10 V SINIS Josephson arrays for programmable voltage standards *Supercond. Sci. Technol.* **13** 1293–5
Schulze H, Behr R, Müller F and Niemeyer J 1998 $Nb/Al/AlO_x/Al/Nb$ Josephson junctions for programmable voltage standards *Appl. Phys. Lett.* **73** 996–8
Séron O, Djordjevic S, Budovsky I, Hagen T, Behr R and Palafox L 2012 Precision ac–dc transfer measurements with a Josephson waveform synthesizer and a buffer amplifier *IEEE Trans. Instrum. Meas.* **61** 198–204
Shapiro S 1963 Josephson currents in superconducting tunneling: the effect of microwaves and other observations *Phys. Rev. Lett.* **11** 80–2
Stewart W C 1968 Current–voltage characteristics of Josephson junctions *Appl. Phys. Lett.* **22** 277–80
Taylor B N, Parker W H, Langenberg D N and Denenstein A 1967 On the use of the ac Josephson effect to maintain standards of electromotive force *Metrologia* **3** 89–98
Toonen R C and Benz S P 2009 Nonlinear behavior of electronic components characterized with precision multitones from a Josephson arbitrary waveform synthesizer *IEEE Trans. Appl. Supercond.* **19** 715–8
Urano C *et al* 2010 A new coding technique in serial data transmission and demodulation with Josephson junctions array *J. Phys.: Conf. Series* **234** 042037
van den Brom H E and Houtzager E 2010 Minimizing voltage lead corrections for a pulse-driven Josephson voltage standard *Conf. Digest CPEM 2010* pp 6–7
van den Brom H E, Houtzager E, Brinkmeier B E R and Chevtchenko O A 2008 Bipolar pulse-drive electronics for a Josephson arbitrary waveform synthesizer *IEEE Trans. Instrum. Meas.* **57** 428–31
van den Brom H E, Houtzager E, Verhoeckx S, Martina Q E V N and Rietveld G 2009 Influence of sampling voltmeter parameters on rms measurements of Josephson stepwise-approximated sine-waves *IEEE Trans. Instrum. Meas.* **58** 3806–12
Waltrip B C, Gong B, Nelson T L, Wang Y, Burroughs C J, Rüfenacht A, Benz S P and Dresselhaus P D 2009 AC power standard using a programmable Josephson voltage standard *IEEE Trans. Instrum. Meas.* **58** 1041–8
Warnecke P, Niemeyer J, Dünschede F W, Grimm L, Weimann G and Schlapp W 1987 High-precision resistance ratio measurements by means of a novel Josephson potentiometer *IEEE Trans. Instrum. Meas.* **36** 249–51
Watanabe M, Dresselhaus P D and Benz S P 2006 Resonance-free low-pass filters for the AC Josephson voltage standard *IEEE Trans. Appl. Supercond.* **16** 49–53
Williams J M, Henderson D, Patel P, Behr R and Palafox L 2007 Achieving sub-100-ns switching of programmable Josephson arrays *IEEE Trans. Instrum. Meas.* **56** 651–4
Williams J M, Henderson D, Pickering J, Behr R, Müller F and Scheibenreiter P 2011 Quantum-referenced voltage waveform synthesiser *IET Sci. Meas. Technol.* **5** 163–74
Williams J M, Janssen T J B M, Palafox L, Humphreys D A, Behr R, Kohlmann J and Müller F 2004 The simulation and measurement of the response of Josephson junctions to optoelectronically generated short pulses *Supercond. Sci. Technol.* **17** 815–8
Witt T 2005 Investigations of noise measurements of electronic voltage standards *IEEE Trans. Instrum. Meas.* **50** 567–70
Wood B and Solve S 2009 A review of Josephson comparison results *Metrologia* **46** R13–20
Yamamori H, Ishizaki M, Shoji A, Dresselhaus P D and Benz S P 2006 10 V programmable Josephson voltage standard circuits using $NbN/TiN_x/NbN/TiN_x/NbN$ double junction stacks *Appl. Phys. Lett.* **88** 042503
Yamamori H, Yamada T, Sasaki H and Shoji A 2008 10 V programmable Josephson voltage standard circuit with a maximum output voltage of 20 V *Supercond. Sci. Technol.* **21** 105007